Liquid Metal Infiltration Processing of Metallic Composites: A Critical Review

K.M. SREE MANU, L. AJAY RAAG, T.P.D. RAJAN, MANOJ GUPTA, and B.C. PAI

Metal matrix composites (MMC) are one of the advanced materials widely used for aerospace, automotive, defense, and general engineering applications. MMC can be tailored to have superior properties such as enhanced high-temperature performance, high specific strength and stiffness, increased wear resistance, better thermal and mechanical fatigue, and creep resistance than those of unreinforced alloys. To fabricate such composites with ideal properties, the processing technique has to ensure high volume fraction of reinforcement incorporation, uniform distribution of the reinforcement, and acceptable adhesion between the matrix and the reinforcing phase without unwanted interfacial reactions which degrades the mechanical properties. A number of processing techniques such as stir casting/vortex method, powder metallurgy, infiltration, casting *etc*. have been developed to synthesize MMC employing a variety of alloy and the reinforcement's combinations. Among these, infiltration process is widely used for making MMC with high volume fraction of reinforcements and offers many more advantages compared to other conventional manufacturing processes. The present paper critically reviews the various infiltration techniques used for making the MMC, their process parameters, characteristics, and selected studies carried out worldwide and by authors on the development of metal ceramic composites by squeeze infiltration process.

DOI: 10.1007/s11663-016-0751-5

I. INTRODUCTION

LIQUID metal infiltration of ceramic preform is apparently the best suited fabrication method to produce metal matrix composite components with variety of complex shapes having high volume fraction of reinforcement. Infiltration is a liquid-state fabrication method, in which a porous preform (reinforcement) such as ceramic particles, fibers, woven *etc*. are impregnated in a molten matrix metal, which fills the pores between the dispersed-phase inclusions. Synthesis of porous ceramic preform with sufficient mechanical strength, uniform pore distribution, pore size, and porosity level is one of the crucial steps involved in the infiltration processing of composites.[1,2] The captivating properties of these ceramic foams such as thermal resistance, low density, controlled permeability, low thermal conductivity, high surface area, and high structural uniformity make them potential candidates for multiple engineering applications.[3,4] Some of the important fabrication methods for porous ceramic foams are polymer replica techniques, gel casting, direct foaming of suspensions, and using pore-forming agents (PFA).[5–11] Al-, Mg-, and Cu-based alloys have been successfully used as matrices to contrive MMCs through liquid infiltration, as they can be easily melted and handled in the liquid state. Difference from one infiltration method to another is based on the technique that is used to drive the molten metal to enter the preform. The present paper gives the state-of-art knowledge on the various infiltration processing methods of MMCs and their characteristics. The investigations carried by the authors at NIIST, Trivandrum, India on infiltration processing of the metal matrix composites using porous ceramic preform are also described.

II. METALLIC COMPOSITES

The inclusion of high strength and modulus ceramic reinforcements to a ductile metal matrix forms the metallic composites having unique combination of properties offering high resilience, high-temperature applications compared to polymer and ceramic matrix composites. From tribological perspective, the addition of hard ceramic reinforcements increases the wear resistance of the metallic matrix. Ultimate combination of properties of MMCs depends on a number of factors related to matrix, reinforcement, processing, and heat treatment. Samer *et al*. recommended that the young's modulus, UTS, and maximum elongation of the composite depends on the particle size of the reinforcements

K.M. SREE MANU, Senior Research Fellow, and T.P.D. RAJAN, Senior Scientist, are with the Materials Science and Technology Division, CSIR-National Institute for Interdisciplinary Science and Technology, Trivandrum, India, and also with the Academy of Scientific and Innovative Research, New Delhi, India. Contact e-mail: tpdrajan@gmail.com L. AJAY RAAG, Research Scholar, and B.C. PAI, Emeritus Scientist, are with the Materials Science and Technology Division, CSIR-National Institute for Interdisciplinary Science and Technology. MANOJ GUPTA, Professor, is with the Department of Mechanical Engineering, National University of Singapore, Singapore, 119260, Singapore.

Manuscript submitted February 26, 2016.
Article published online July 14, 2016.

and obtained superior properties in composites containing nanoparticles (~70 nm) when compared to composites containing micrometer range particles in Al/TiC system.[12] Formation of ductile intermetallic phases during solidification and potential of the material to be strengthened by precipitation are considered as distinct advantages in metallic composites, which empower the mechanical properties of the composite.

The properties of the MMCs are also determined by the type and morphology of reinforcement incorporated in the molten metal matrix-like particulates, whiskers, continuous fiber, discontinuous fiber, *etc.* Aluminum, magnesium, and titanium alloys are the most commonly used matrix materials for MMC processing due to their low specific gravity and those find wide range of applications in automotive and aerospace sectors. In metallic composites, the thermal stress caused due to thermal mismatch between matrix and reinforcement can be reduced from the matrix plastic deformation phenomena.[13] Nowadays, fabrication of MMC focuses on nanocomposites where the matrix alloys are coupled with nanoparticle reinforcements like carbon nanotubes, SiO_2, Y_2O_3, SiC, Al_2O_3, graphene, *etc.*[14,15]

III. PREFORM MATERIALS

The porous ceramic preforms contemplate as scaffolding, are considered to be the base of the composite materials processed by infiltration technique. The properties of the composite depend on the strength, distribution, type, and structure of the interconnected pores in the porous body to facilitate the liquid metal infiltration. Thus, the process parameters have to be optimized for synthesizing quality composites. Assorted type of fundamental works by varying the processing, pore former (NaCl, PEG, carbon fiber, tylose), reinforcement (Al_2O_3, SiC, Si_3N_4), and binding agent (aluminum, poly vinyl alcohol) have been carried out by several investigators. However, the depth and speed of the infiltration is influenced by the coefficient of permeability in the preform, which alters with the volume fraction of reinforcement. Yamanaka *et al.*[16] concluded that the temperature, wettability, and the volume fraction of reinforcement in the preform regulate the coefficient of permeability in the system. An increase in the volume fraction of reinforcement reduces the gaps and open porosity in the porous preform, which reduces the ability of the liquid molten metal to get penetrated. Based on the experimental studies it is found that the permeability k of a porous preform is directly proportional to the square of the mean diameter of the reinforcement.[17]

$$k = aD^2, \qquad [1]$$

where a is the constant which depends on the reinforcement morphology. Dobrzanski *et al.*[18] fabricated Al_2O_3-based preforms using carbon fiber as the pore-forming agent and observed the increase of permeability with an increase in pore former content.

The strength of the porous preform is negatively affected by increasing the pore former content because it increases the porosity level and by randomness in distribution of pores. In accordance with the above factor, nonuniform distribution of pores in the preform will create difference in the collateral wall thickness and cause inability to withstand localized stress concentration resulting in deformation.[19] The grain size of the particles has great impact on the porosity hike and strength of the preform. Increase in the grain size is inversely proportional to the mechanical strength of the preform owing to low diffusion on grain boundaries.[20] The morphology of the pores in the preform depends on the kind and type of pore former used in the system. Raddatz *et al.*[21] created hollow channels in the ceramic preform by integrating cylindrical-shaped polymer fibers as pore-forming agent. The binding agent in the preform plays a dual role, which imparts strength to the green body as well as the sintered porous structure by bridging between the particles. Moreover, the selected binder should not pave way for the interfacial reactions with the reinforcement and molten metallic matrix during infiltration. Mechanical strength of the porous preform basically depends on the kind and the type of binding agent used for fabrication; metallic binders can be used for partial coating on reinforcements to improve wettability.

IV. PROCESSING TECHNIQUES

The liquid infiltration processes can be broadly classified into two categories: (a) spontaneous infiltration and (b) forced infiltration (Figure 1). When capillary action of the reinforcement phase acts as a driving force for infiltration, the category of processes is termed as spontaneous infiltration. In forced infiltration an external pressure such as gaseous, mechanical, squeeze, electromagnetic *etc.* are applied to the liquid matrix phase which accelerates the infiltration of molten metal through the preforms. The processing details are briefly discussed here.

A. *Spontaneous/Pressure-Less Infiltration*

In spontaneous infiltration, the molten liquid metal invades into the voids of the porous body without the application of any external forces (Figure 2).[22–27] This can be accomplished with the help of controlled temperature and gas atmosphere ensuring good wetting conditions are maintained for self-permeation.[28] Numerous studies in pressure-less infiltration have been carried out using Al-Si, Al-Zn, Al-Mg alloys into porous SiC preform and however, there are some challenges that should be tackled to develop spontaneous infiltration a very promising and industrially adaptable method. Conventional drawback of the infiltration synthesis method is the poor wettability between the matrix and the reinforcement resulting from the formation of oxide layer on the melt surface.[29] Poor wettability negatively influences the infiltration process by slowing down the infiltration process leading to undesirable reactions at

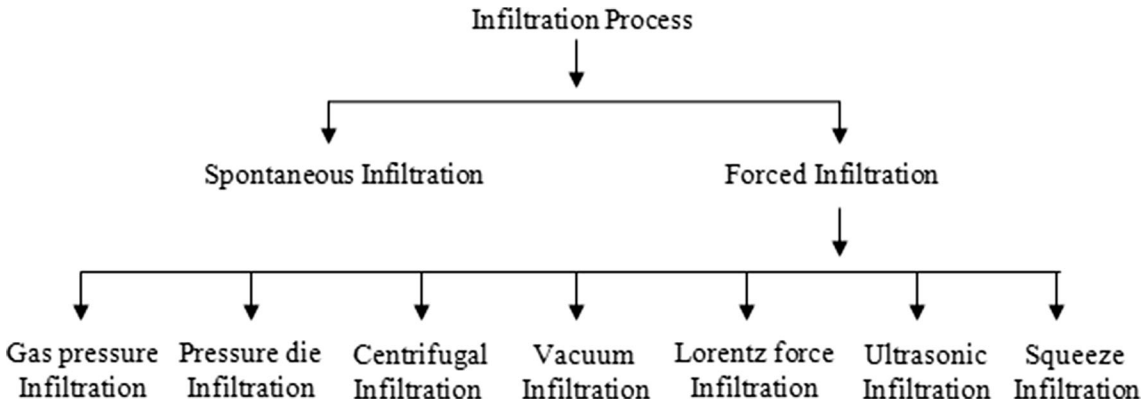

Fig. 1—Classification of infiltration process for the fabrication of metal matrix composites.

the interface resulting in the formation of intermetallics such as Al_4C_3 and Al_3SiC_4 in aluminum-SiC-based systems.[30] Many researchers had investigated the effect of activator content in pressure-less infiltration of metal matrix composites.[31] Dwell time and activator primarily controls the rate of infiltration. More the activation more will be the infiltration depth. The amount of porous areas and residual porosity also govern the infiltration quality but this can be reduced by increasing the activator content.[32] The wettability of preform by liquid molten metal is an essential parameter for processing composites by pressure-less infiltration technique. Wittig *et al*. suggests that the addition of titanium in the steel matrix composites reinforced with ZrO_2 particles helps in improving the wetting behavior of liquid metal to ceramic preforms.[33] Contreras *et al*. successfully infiltrated liquid magnesium into TiC preforms by pressure-less technique.[34] Previous studies suggest that the wettability can be improved by adding 3-4.7 mass percent of magnesium to the melt and also using 100 pct nitrogen atmosphere in the furnace.

Magnesium is known to be a powerful surfactant that accumulates oxygen from the surface of the melt and forms $MgAl_2O_4$ spinel at the interface. The reaction results in attenuating the oxide layer and acts as driving force to promote wetting.[35] Schiroky *et al*. reported the PRIMEX™ pressure-less infiltration process of SiC and alumina infiltration by Al-Mg alloy. During the pressure-less infiltration process, the Mg in the Al-Mg alloy at 800 °C vaporizes and reacts with the nitrogen gas used as atmosphere for the process to form Mg_3N_2 and deposits on the reinforcement surface. During aluminum alloy infiltration, Al reacts with Mg_3N_2 to form AlN and Mg which promotes better wetting with the reinforcement.[36] Even though, the primary motive for the use of nitrogen during infiltration is the prevention of Al alloy oxidation it aids in reinforcement wetting also. The effective chemical reaction between the constituents in the molten metal and trapped gases in the porous preform causes pressure drop in the preform and thereby improves the ease of molten metal penetration. Nake *et al*. studies the spontaneous infiltration mechanism of Al-Si-Mg alloy on SiC preform with the addition of Fe_2O_3 in the preform as additives to improve wettability. The pressure reduction in the preform improves the suction of the molten metal which helps to break the oxide film present at the interface between the metal and the preform (Figure 3) formed due to the reaction between the molten metal and the adsorbed moisture at the infiltration front.[37]

Generally, the wetting system of solid by a liquid is stipulated by contact angle (Figure 4) and the contact angle, θ, at the solid, liquid, and gas/vapor is related by the Young–Dupre's equation.[38]

$$\gamma_{lv} cos\theta = \gamma_{sv} - \gamma_{sl}, \qquad [2]$$

where γ_{lv}, γ_{sv}, and γ_{sl} are the liquid metal surface tension, surface energies of solid/vapor and solid/liquid, respectively. The molten metal will wet the solid preform, if $\gamma_{sv} > \gamma_{sl}$, that is, when $\theta < 90$ deg. Similarly, if the above process is reverse in the case of nonwetting system a minimum pressure (threshold pressure) is to be exerted for infiltration. As stated by Darcy's law, the infiltration rate of molten metal into porous preform is[39]

$$v = \frac{k}{\mu}\frac{dp}{dx}, \qquad [3]$$

where v is the flow rate, k is the permeability which depends on the shape and sizes of the interconnected channels through which the molten metal flows, μ is the viscosity of the molten metal, p is the pressure (capillary pressure for spontaneous) correlated with the size and shape of the pores that are in contact with the molten metal, and x is the infiltration distance. Surface modification of reinforcements is also an effective method to circumvent interfacial reactions and enhance wetting. Treatments include metallic coatings like Cu, Ni, Zn, Ag, Si *etc*. and high-temperature treatment, for example, of SiC leads to the formation of very stable surface layer of amorphous silica.[40,41] It has also been reported that the coating of K_2ZrF_6, ZrO_2, and Na_2O in the fillers helps pressure-less infiltration.[42–44] Continual investment and further process optimization can ensure spontaneous infiltration techniques to remain an attractive technique to synthesize composites in the time to come.

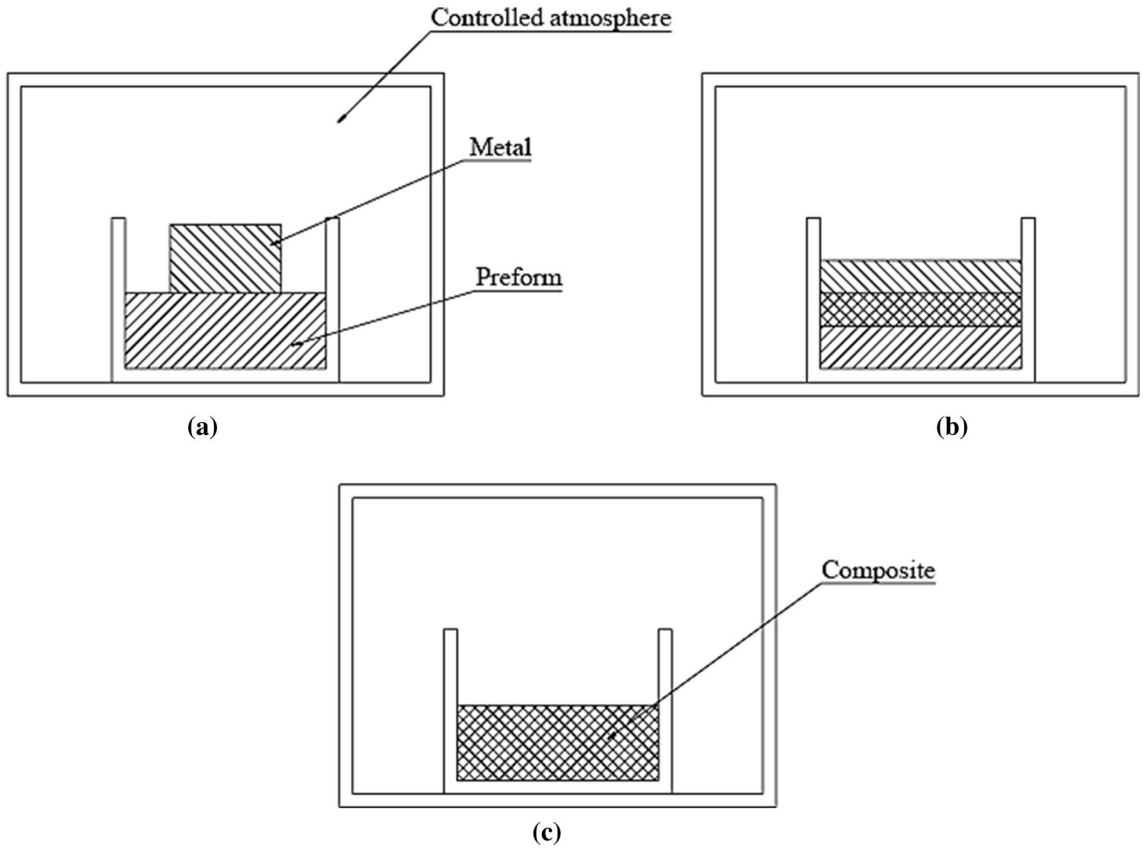

Fig. 2—Schematic diagrams showing the working principle of spontaneous infiltration process: (*a*) infiltration takes place at controlled atmosphere, (*b*) progressiveness of infiltration, and (*c*) final composite.

B. *Forced Infiltration*

The infiltration process in which the aid of an external pressure or mechanical force governs the infiltration of liquid metal into the porous reinforcement is called forced infiltration. Poor wetting between the molten metal and porous structure can be overcome by endowing mechanical energy to force the metal into the porous preform. There are various types of forced infiltration methods and these are described below.

1. *Gas pressure infiltration*

An infiltration process in which pressurized gas (Figure 5) is used as driving force for the penetration of molten metal into the porous body. Gas infiltration process is normally carried out in combination with vacuum at the other end of the preform to get rid of entrapped air to facilitate easy penetration at lower gas pressures.[45] Qi *et al.* suggests that the antipressure of gas in the porous preform significantly slows down the rate of infiltration, which increases with increase in infiltration depth and the temperature. As a result high pressure is needed for complete infiltration of molten metal, hence, antipressure of gases is to be considered during the analysis of threshold pressure. With the ideal gas equation $PV = nRT$, the antipressure of gas can be expressed as[46]

$$p_g(z) = \frac{p_0 T_Z L}{T_0[L - z]} \quad [4]$$

where p_0 is the pressure of gas at initial time, T_0 is the initial time temperature, L is the preform total length, and T_z is the temperature of the gas when the infiltration attains a height z. Enhance in the infiltration temperature and pressure during gas pressure infiltration process improves the relative density of the component, which shows an effect on the mechanical properties of the final composite.[47] Joseph Blucher concluded that the fabrication of MMC by hydrostatic gas pressure infiltration holds certain advantages like low acquisition cost, high operational flexibility for research purposes *etc.*[48] Al alloys reinforced with Ni- and Cu-coated chopped, unidirectional carbon fibers and porous graphite preforms were successfully fabricated using gas pressure infiltration technique.[49–51] Non-coated fibers can also be used in gas pressure infiltration technique due to the short contact time of the matrix with the reinforcement. Drawback of the gas infiltration technique is the added cost of pressurized gas which usually is an inert gas.

2. *Pressure die infiltration*

Pressure die infiltration process involves placing a porous preform inside a solid die and applying pressure

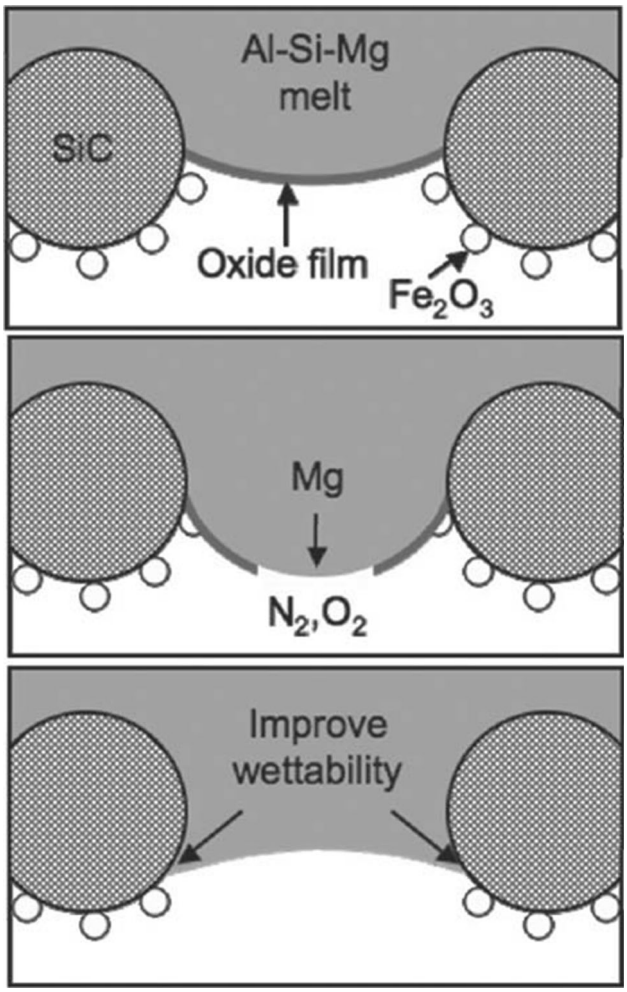

Fig. 3—Schematic diagram showing the penetration of molten metal into the SiC preform by breaking the oxide film at the interface during spontaneous infiltration. Reprinted from Nakae *et al.*[37] with permission from Springer.

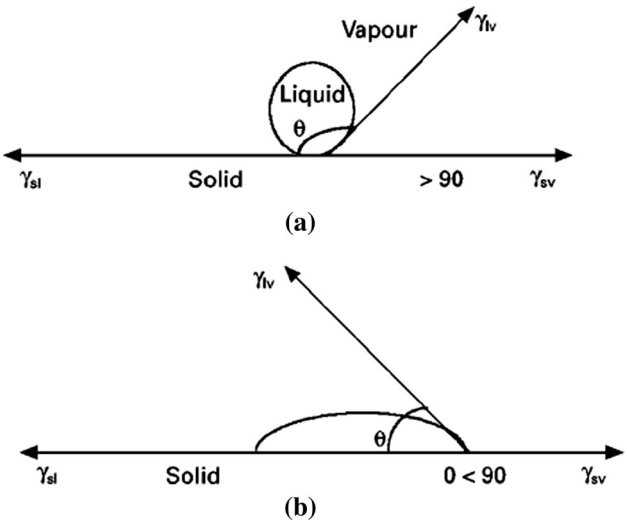

Fig. 4—Schematic illustrations showing the contact angle in a (*a*) nonwetting system and (*b*) wetting system.[38]

with the help of a movable piston to allow penetration of liquid metal in the porous preform (Figures 6(a) and (b)). Process parameters that are optimized include speed, die temperature, and pressure of the piston. Main advantages of this process are low cost and ability to fabricate components of high complexity and precision. The deformation of preform due to the pressure of the molten metal before and during infiltration will be high for pressure die casting compared to squeeze casting owing to high compression rate of preform during infiltration. Rasmussen *et al.* suggests that by increasing the volume fraction of the reinforcement leads to stronger preform which can prevent preform deformation, but at the same time it will prohibit the ease of infiltration.[52]

3. *Centrifugal infiltration*

In centrifugal infiltration process, rotational/centrifugal force is used to infiltrate porous preform with liquid molten metal. During the fabrication of composites, porous reinforcement material is positioned inside a mold (at the end) having an elongated runner, which was filled with molten metal. Large rotational velocities of the runner initiate centrifugal force with required drive for infiltration to overcome the threshold pressure for melt penetration and viscous forces of the molten metal to flow in the preform. The molten metal pressure exerted on the porous preform during centrifugal force is given by[53]

$$p_c = \frac{1}{2}\rho\omega^2\left(L_2^2 - L_1^2\right), \qquad [5]$$

where ρ is the density of molten metal, $= \frac{2\pi\Omega}{60}$, Ω is the rotational speed in rpm, and L_2 and L_1 are the outer and the inner molten metal's level from the rotation axis. To develop the near net shape components and to avoid the material wastage typical centrifugal infiltration technique is adopted (Figure 7(a)). In order to achieve high pressure centrifugal infiltration, a slight modification within the same centrifugal system used for conventional process is made by extending the inner molten metal level L_1 from the rotational axis (Figure 7(b)). In such cases liquid metal pressure acting on the preform will be given by

$$p_c = \frac{1}{2}\rho\omega^2 L_2^2 \qquad [6]$$

Surface-coated and noncoated carbon short fiber preforms were successfully infiltrated by centrifugal process and the optimum preform preheating temperature for noncoated fiber for the smooth penetration of molten metal is above 873 K (600 °C), whereas for nickel-coated carbon fiber preform is 673 K (400 °C).[54] In addition, surface pressure of the porous preform is reduced perceptibly as the molten metal starts to infiltrate and once when the metal gets penetrated into the preform the pressure of the infiltrated region falls under the threshold pressure. The adhesion between the molten metal and the reinforcement will not get separated due to the fall of pressure in the infiltrated zone below the threshold pressure. However, to achieve a

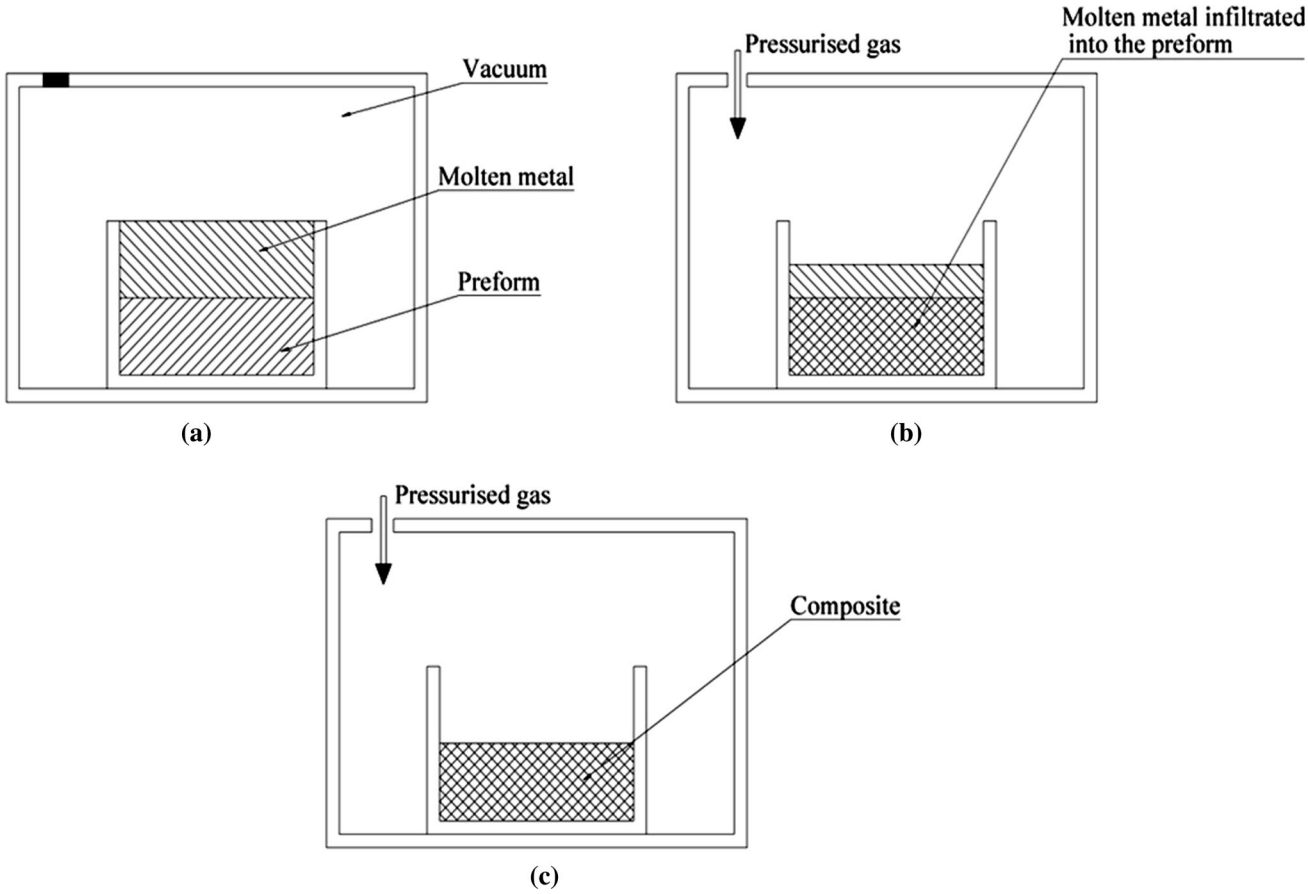

Fig. 5—Schematic illustrations of gas pressure infiltration process for the fabrication of MMCs: (*a*) infiltration process carried out with vacuum to remove the entrapped air in the preform to facilitate easy molten metal penetration, (*b*) applying pressurized gas as a driving force for metal infiltration, and (*c*) final composite.

complete infiltration of molten metal throughout the porous preform, the pressure on the infiltration front should exceed the threshold pressure.[55]

4. *Lorentz force infiltration*

Lorentz force infiltration process is a novel infiltration process in which electromagnetic force is used to propel the molten metal into the ceramic preforms. During the process, the preform gets immersed in a liquid molten metal which is subjected to an high-frequency magnetic pulse. Simultaneously, eddy current persuaded in the liquid metal gets to interact with the magnetic pulse and develop a Lorentz body force in the liquid molten metal causing the liquid metal to enter into the ceramic preform at a high speed. Richard M. Andrews and Andreas Mortensen had successfully fabricated void-free aluminum/Al_2O_3 fiber composite by Lorentz force infiltration technique. They suggested that the infiltration depth depends on the nature and number of discharges.[56]

5. *Ultrasonic infiltration*

In ultrasonic infiltration process, pressure waves generated by the ultrasonic vibration assist in the penetration of the molten matrix material in the ceramic preform. When ultrasonic vibration is actuated through a horn in the liquid molten metal, acoustic cavitations (bubbles) are originated. The air entrapped in the porous preform and the dissolved gas in the molten metal can become the cavitations' nuclei. When a bubble collapses shock wave originates close to the molten metal resulting in infiltration process (Figure 8).[57,58]

The important process parameters considered for the ultrasonic infiltration is ultrasonic power, hole in the horn, and fabrication speed. Increase in the diameter of the hole in the horn decreases the infiltration ratio due to the depletion in the formation of acoustic cavitations and studies show that optimum diameter of the hole is 5 mm. Studies have shown that the infiltration can be made more effective by the addition of 2.4 mass pct magnesium to liquid Al metal coupled with an ultrasonic power of 200 W. Similarly, infiltration ratio decreases with increase in the fabrication speed, but at the same time addition of magnesium in the molten metal for wettability helps to increase the fabrication speed with better infiltration ratio.[59,60] Gen sasaki *et al.* studied the effect of ultrasonic vibration on the wettability during infiltration using contact angle technique of polyester resin on glass substrate with and without ultrasonic vibration (Figure 9). The system which undergoes ultrasonic vibration shows reduction in contact angle due to heavy vibration acceleration and thereby improving wettability.[61]

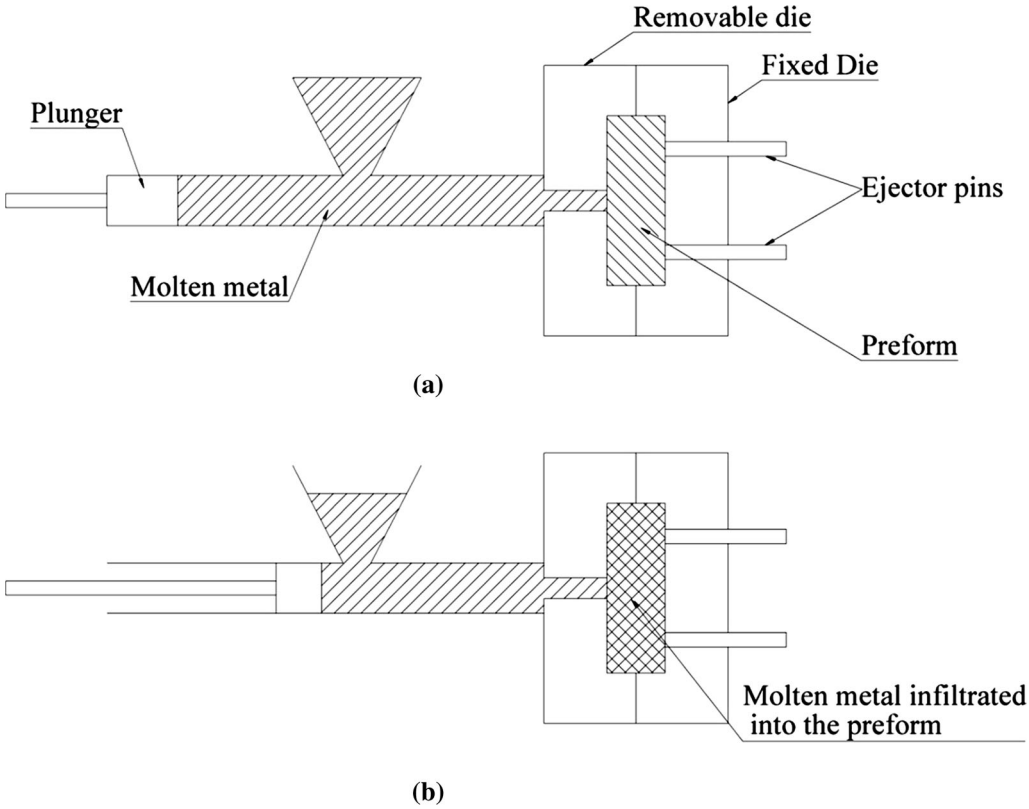

Fig. 6—Schematic diagrams of pressure die infiltration process for the fabrication of MMCs: (*a*) before applying pressure to molten metal using plunger and (*b*) after applying pressure to molten metal using plunger to form the composite.

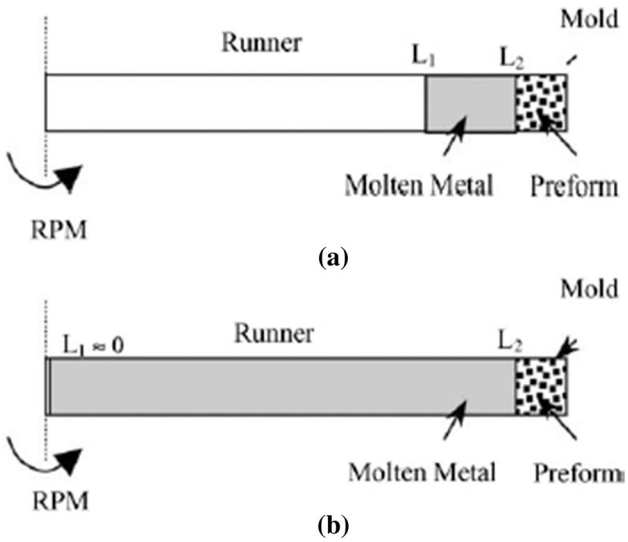

Fig. 7—Schematic diagrams of (*a*) a traditional centrifugal infiltration process and (*b*) a high pressure centrifugal infiltration process. Reprinted from Wannasin *et al.*[53] with permission from Elsevier Limited.

6. *Vacuum infiltration*

Vacuum infiltration involves a negative pressure infiltration in which matrix metal gets penetrated into the evacuated preform due to the application of suction pressure (Figure 10). Process parameters like infiltration temperature, infiltration time, and applied vacuum (~300 to 500 mmHg) play a crucial role in this process.[62] Infiltration rate gets increased with increasing the molten metal temperature and by applying coating on the reinforcement, thereby reducing the infiltration incubation period to avoid brittle interfacial reactions.[63] Low solidification rate of the final component during processing can be stepped up as one of the disadvantage of vacuum infiltration which enhances the grain growth of the matrix metal and interfacial reaction between matrix and the reinforcement.[64] To avoid the liquid molten metal getting into the vacuum pump by chance during infiltration process one portion of the connection pipe is filled with metal chips, so that the molten metal entering into the pipe gets solidified in that particular area without damaging the vacuum pump. Studies have shown that Al- and Mg-based composite materials with more than 50 vol pct reinforcement can be successfully fabricated using vacuum infiltration technique.[65]

7. *Squeeze infiltration*

Squeeze infiltration is one of the widely used methods for the production of near net shape metal matrix composites with close control over shape, volume fraction, chemistry, and distribution of reinforcement.[66–72] This process offers advantages over other conventional methods for fabricating composite components which are difficult to be machined. The process involves the formation of porous preform as the reinforcement and its infiltration with the molten matrix

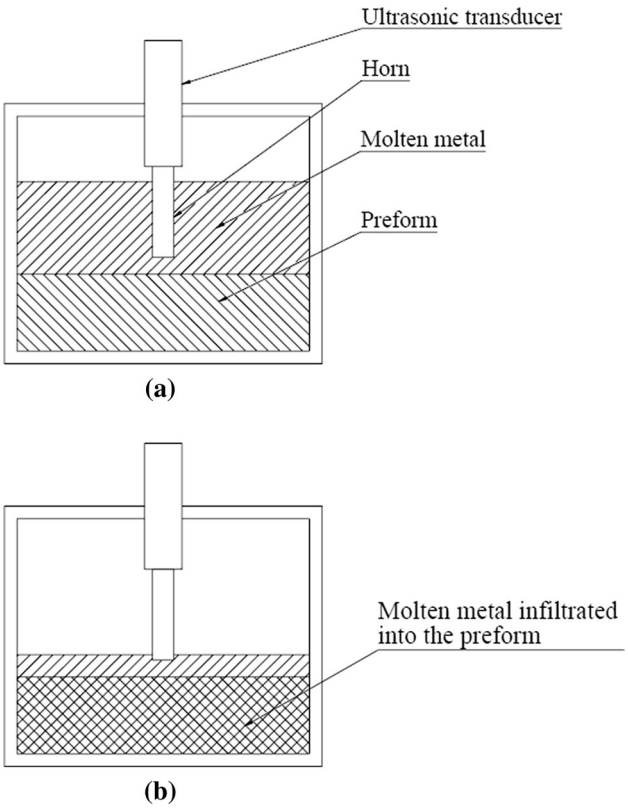

Fig. 8—Schematic diagrams of ultrasonic infiltration process for the fabrication of MMCs: (*a*) before ultrasonic vibration and (*b*) after ultrasonic vibration using transducer as a driving force to penetrate molten metal into the ceramic preform.

material under pressure (Figure 11) typically in the range of 50-100 MPa.[22] The appropriate magnitude of applied pressure ensures eradication of porosities, refined microstructure, enhanced processing speed, and termination of chemical reactions. For the development of quality composites processing parameters of squeeze infiltration have to be optimized.

In light of the above, the application of higher squeeze pressure accelerates the infiltration process but leads to crumpling or cracking of the porous preform. Numerous studies regarding infiltration pressure have been done by many researchers. Guan *et al.*[73] investigated the threshold pressure and infiltration behavior of liquid metal into the porous preform. The infiltration rate can be improved effectively by raising infiltration pressure, but the effect will gradually diminish with the advancement in time. Increase in infiltration pressure minimizes porosity, reduces the heat loss, and hinders the solidification of liquid metal front effectively. According to Darcy's law, the expression for the square of infiltration height as a function of infiltration time and difference in infiltration pressure of the liquid metal is[74]

$$h^2 = \frac{2kt}{\mu(1 - V_s)}(p - p_0), \qquad [7]$$

where p is the applied pressure, p_0 is the threshold pressure for the initiation of infiltration, infiltration time t, μ is the viscosity of molten metal, v_s is the volume fraction of solid, and k is the permeability of the porous solid. The threshold pressure p_0 for infiltration can be obtained as[75]

$$p_0 = 6\lambda\gamma_{lv}\cos\theta\frac{V_s}{(1 - V_s)D}, \qquad [8]$$

where λ is a geometrical factor that represents the deviations from particle/fiber shape, surface roughness, and actual particle/fiber size distribution. The basic governing phenomenon for the infiltration of metals, ceramics, and polymers into the porous preforms are fluid flow, capillarity, and the behavior of preform deformation, which in turn are decided by preform permeability, volume fraction of reinforcement, preform stress–strain behavior, pressure-dependant saturation of melt in the porous preform, and the melt viscosity.

The strength and stability of preform during infiltration depend on the mode of fabrication of preform, type of binder, and the reinforcement used. Reinforcements having lubrication nature enhance the tendency of sliding over one another thereby increasing the chance for deformation of the preform. Similarly during the fabrication of layered preform, equality in the stacked layers reduces the preform compliance.[76] A new technique for the direct measurement of capillary force is by drainage curve method through which the corresponding volume fraction of the molten metal in the porous preform as a function of applied pressure is plotted and the method adopted is also suitable for measuring contact angle and infiltration kinetics.[77] Higher temperatures of liquid metal, preform, and die initiate unwanted chemical reactions at liquid metal/fiber interface and prolong the solidification time.[78] Delaying the application of pressure after pouring the molten metal above preform in the mold causes the formation of oxide layer around the preform, which decelerates the infiltration process.[79] Oxide inclusions, porosity and voids, blistering, cold laps and cold shuts, and sticking of casting with the die surface are the major casting defects that occur in the squeeze cast process.[80] Alhashmy *et al.* processed carbon fiber-reinforced aluminum matrix composite by squeeze infiltration technique.[81] They suggested that the inclusions can be avoided using filters and turbulence must also be completely avoided while pouring. Porosity can be avoided by increasing the squeeze pressure. The main cause for blistering is the entrapment of gas from the melt and can be avoided by reducing the pouring temperature and degassing the melt. Die temperature and metal pouring temperature can be increased to avoid cold laps and better lubrication or die coating to avoid sticking of casting with the die surface.

V. SQUEEZE INFILTRATION OF ALUMINUM MMC AND FGM

Squeeze infiltration processing setup for Al MMC has been designed and developed at CSIR-NIIST. During squeeze infiltration parameters like the design of die, the

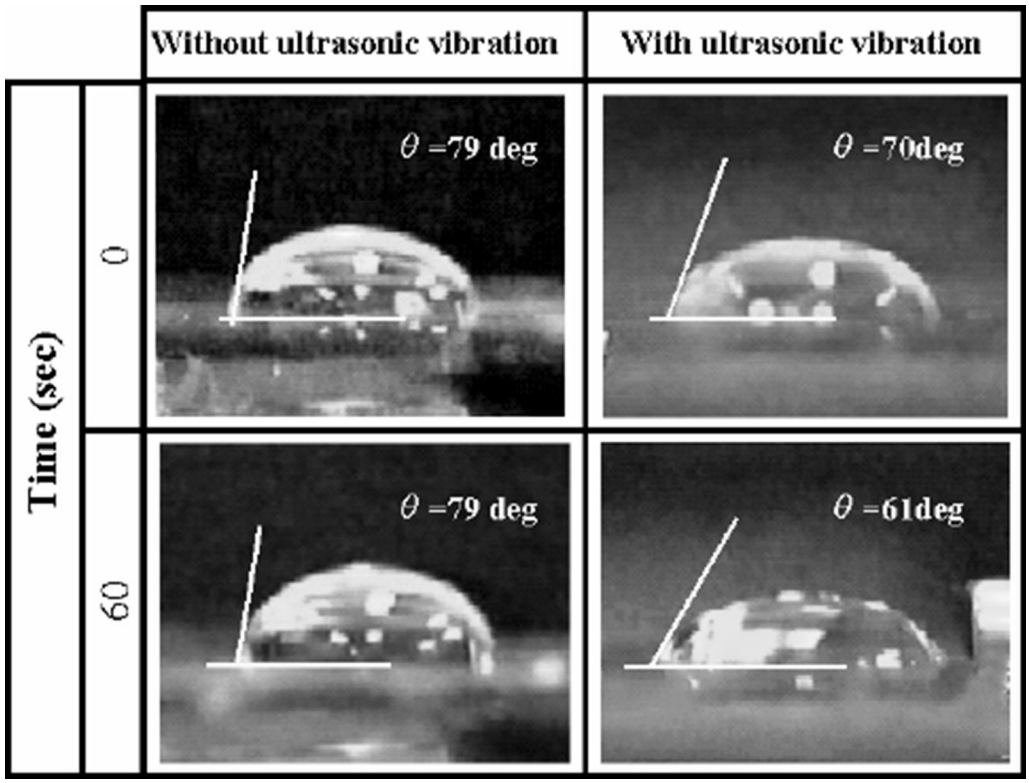

Fig. 9—Effect of ultrasonic vibration on contact angle. Reprinted from Gen Sasaki *et al.*[61] with permission from Trans Tech Publications Limited.

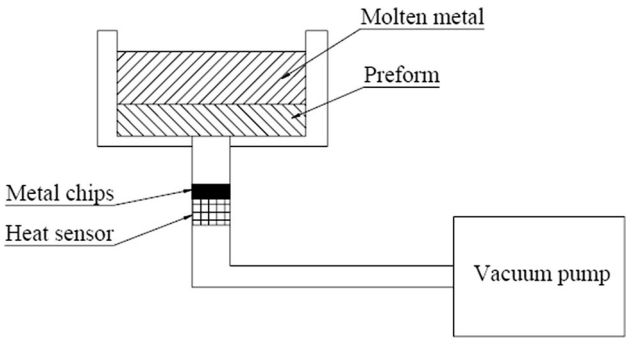

Fig. 10—Schematic diagram showing the working principle of vacuum infiltration process for the fabrication of MMCs.

preform preheating temperature, mold and molten metal temperature, and squeeze pressure plays a vital role for the depth of penetration of liquid metal throughout the porous preform. Some of the highlights of the work carried out by the authors are presented here. Silicon carbide porous preform was made by salt leach out technique and aluminum powder as the binder. Porous preform was placed in a die and infiltrated with liquid 6061 alloy. Macrograph of the infiltrated specimen (Al 6061-50 vol pct SiC ~42 μm) and porous preform used for infiltration process are shown in Figure 12(a). It can be rendered from the representation that the components fabricated can also act as a selectively reinforced composite with the eradication of cold shuts, blistering, and other casting defects. Microstructure in Figure 12(b) shows the uniform distribution of SiC particles in the matrix resulted due to the good quality of preform used and the effective penetration of the liquid metal even in minute voids in the preform.[82] These infiltrated composites find potential application for electronic packaging systems and armor materials.

The emerging new generation advanced composites are the functionally graded materials in which properties vary along a specified direction to provide functional performance for the components. The variation in properties is effected through the change in microstructure and/or composition in the required direction. The ability of these tailored materials to replace sharp interfaces manifests in composite materials by gradient interfaces thereby providing smooth transition from ductile matrix metal to hard ceramic phase is an added advantage.[83] The Squeeze infiltration is one of the effective fabrication methods for synthesizing functionally graded materials. Process involves the framing of graded porous ceramic preform with adequate interconnecting porosity and its infiltration with the molten metal under pressure. The gradation in preforms can be obtained by various techniques like the usage of graded particle sizes for green body compaction which leads to the formation of porosity gradient during sintering and also by the use of graded PFA and their volume fractions which creates porosity gradient during the burn out of fugitive pore former while sintering.[84]

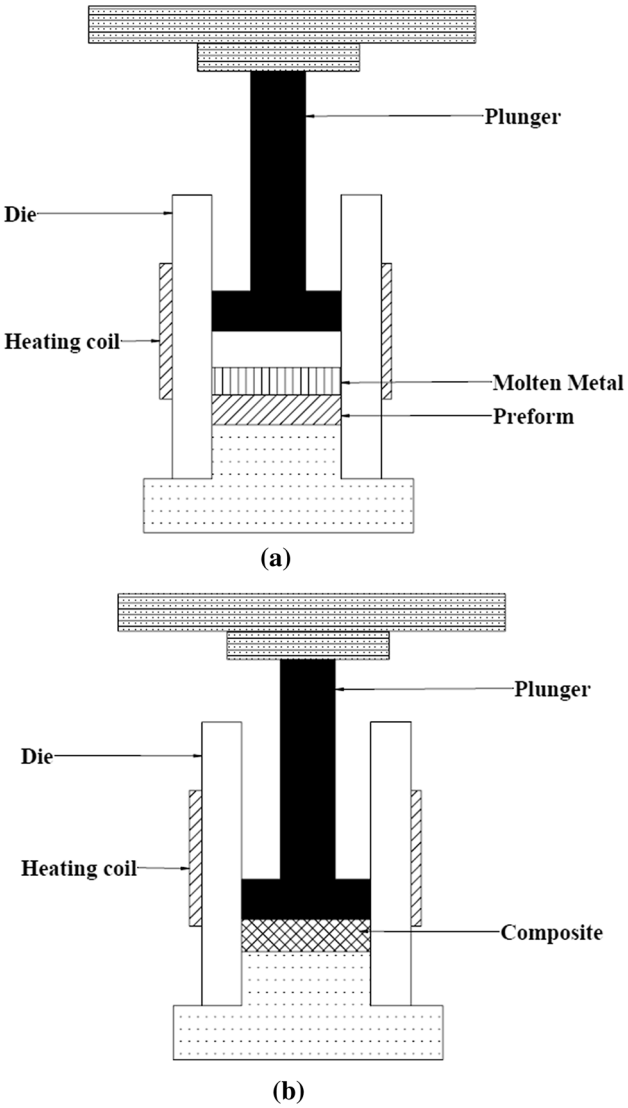

Fig. 11—Schematic diagrams of squeeze infiltration process for the fabrication of MMCs: (*a*) before the application of squeeze pressure and (*b*) after the application of squeeze pressure as a driving force to infiltrate molten metal into the preform.

Figure 13 shows the macrograph and microstructure of functionally graded Al-SiC composite developed by squeeze infiltration method in CSIR-NIIST, India. Macrograph depicts (Figure 13(a)) the graded sintered porous preform (three layers) and its infiltration with Al 6061 molten metal. Microstructure description stipulates the graded distribution of SiC Particles in Al 6061 matrix, starting from outer layer (Figure 13(b)) having high volume fraction of reinforcement (low porosity) to middle layer (Figure 13(c)) having medium volume fraction of reinforcement (medium porosity) and ends in inner layer (Figure 13(d)) having low volume fraction of reinforcement (high porosity) in 12-mm-thick casting. Figure 13(e) shows the interface region between the aluminum 6061 molten metal and the first layer of the preform (from inner side).[85]

VI. CHARACTERISTICS OF INFILTRATED COMPOSITES

A. *Structural Characteristics*

Infiltration-processed composites have more isotropic microstructure compared to other conventional methods due to the use of judiciously designed porous preform as reinforcement. In preform, particles/fibers are tightly packed with binders ensuring regular uniform distribution of pores (pores are artificially created). The aptness to develop complex-shaped components with high volume fraction of reinforcement is an added advantage to the infiltration process compared to other systems. Wetting must be ensured to procure good adhesion between the molten matrix material and ceramic reinforcement especially for spontaneous infiltration processes. Interfacial reactions between the metal matrix and the ceramic reinforcement highly depend on the processing methodology. Preform and die preheat temperature, infiltration pressure, melt pouring temperature, and infiltration time are the major process parameters that govern the infiltration quality. Preform and die preheat temperatures circumvent the sudden solidification of the melt due to lower temperature gradient. More the infiltration time and melt temperature more will be the formation of brittle and undesirable phases like Al_4C_3 (Figure 14). Studies have established that when these kind of components are used in service, carbide phases present in it have the tendency to react with atmospheric moisture to form CH_4 (flammable gas) resulting in porosity and failure of the composite.[86] It may be noted that limited interfacial reactions are desirable and improve the wettability between the matrix and reinforcement thereby enhancing the mechanical properties of the composite.[87–89] During heterogeneous bonding, process temperature and holding time have an impact on the microstructure of the composites prepared by pressure-less infiltration technique. The thickness of the interfacial reaction layer is dominated by the infiltration bonding temperature than the holding time (Figure 15). However, decrease in the holding time causes pores at the interface and these pores can be limited by increasing the holding time.[90]

Matrix alloying is the most appropriate method to enhance the interface bonding strength for continuous carbon fiber-reinforced magnesium matrix composites.[91] The alloying elements are prone to segregation at the interface during the solidification of composites in the form of nanoscale compounds by reacting with matrix or reinforcement. But high quantity of alloying elements may slow down the infiltration rate by reducing the viscosity of the liquid molten metal.[92] Nagendra *et al.* investigated the microstructures and properties of Al_2O_3/Al-AlN composites by pressure-less infiltration of Al alloys.[93] Al_2O_3 was chosen as the preform and liquid aluminum in which AlN is precipitated by nitridation process was selected as the matrix material. They concluded that the processing temperature have a great impact on microstructures. At higher temperature above 1273 K (1000 °C) porosity was observed in the matrix. The presence of AlN at the interface significantly

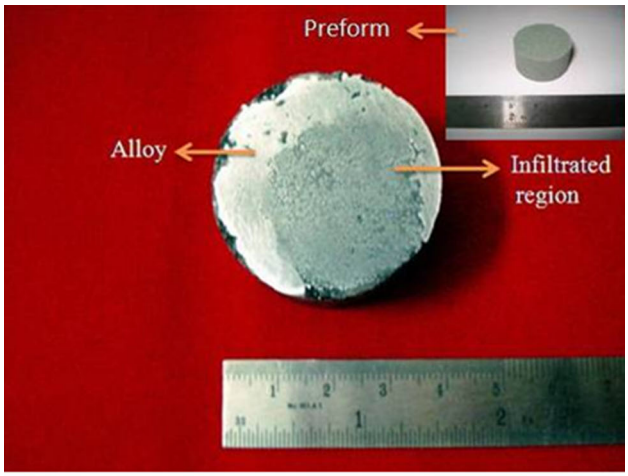

(a)

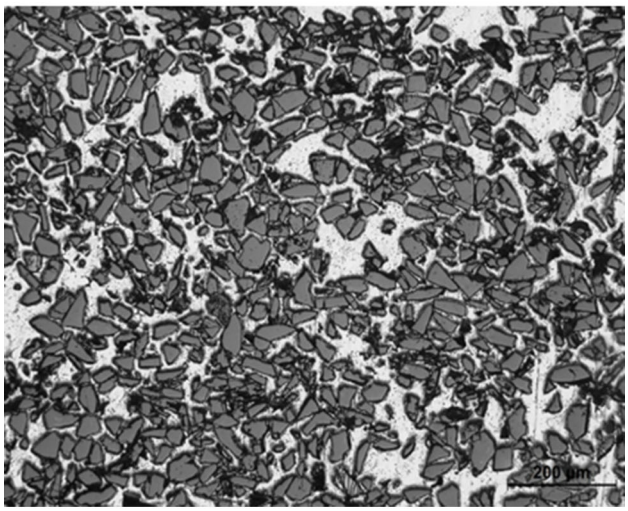

(b)

Fig. 12—Images of (*a*) macrograph of infiltrated specimen and porous preform and (*b*) microstructure of aluminum 6061-50 vol pct SiC-infiltrated composite[82].

improves the hardness and elastic moduli of the composite. In the study done by Zhang *et al*. it was reported that in Cu/SiC composite, the increased infiltration temperature [1698 K (1425 °C)] resulted in the melting of sharp edges of SiC particles (Figure 16) in the preform. The degradation of SiC leads to the releasing of Si and C (black layer around the particle) into the matrix metal.[94]

Warrier *et al*. prepared Ti MMC by rapid infiltration process where the continuous graphite fibers are kept inside a graphite crucible and a calculated quantity of the matrix was placed on top of the fibers. Pressure-less infiltration was carried out at temperatures about 50 °C above the liquidus of the matrix in about 1-2 minutes. Five different alloys ranging from 40 to 85 wt pct Ti showed that the thickness of reaction zone at the matrix/reinforcement interface was found to be increased with increase in the titanium content in the matrix alloy.[95] Matrix–preform interfacial reactions can also be suppressed by nickel coating, SiC coating, copper coating, pyrocarbon coating *etc*. on the preform material especially in the case of carbon fiber preform.[96–101] Dobrzanski *et al*. concluded that the particle-reinforced composite materials synthesized by infiltration process exhibit higher crack resistance along grain boundaries than fiber. The above phenomenon was attributed to the certainty with which each and every particle will act as an obstacle to crack growth. While considering fiber-reinforced composites, propagation of crack will occur over the long distance due to the length of the fiber without any resistance.[102]

B. *Physical Properties*

By decreasing the reinforcement particle size and increasing the volume fraction, low coefficient of thermal expansion composite can be fabricated especially for electronic packaging and structural applications. Etter *et al*. synthesized graphite preform-based composites with pure aluminum and AlSi7Mg alloy as matrix by pressure infiltration technique and the composites were thermally cycled between 333 K and 573 K (60 °C and 300 °C) up to 1020 cycles to investigate their response to thermal damage. The electrical conductivity of the composites was not affected by thermal cycling, however, it reduced the CTE of the composites because of stress relaxation processes. Before thermal cycling, composite with AlSi7Mg alloy as matrix shows higher CTE than the one having pure aluminum as matrix due to the precipitation reaction of Mg_2Si phase at 473 K (200 °C). During thermal cycling Mg_2Si particles were precipitated inside the metal phase of the AlSi7Mg-based composites and thereby show similar CTE values to that of pure aluminum-based composites during the CTE measurement after thermal cycling.[103] Ren *et al*.[104] investigated the effect of adding Mg and Si to aluminum matrix on the physical properties of the SiCp/Al composites processed by pressure-less infiltration. Si content above 12 wt pct retards the interfacial reactions between alloy and SiC by precipitating at the interface (Figure 17). Formation of reaction product Al_4C_3 needles at the interface between the Al-SiC is observed in Figure 17(a) without the addition of Si. Increase in the silicon content eliminates the interfacial reaction products thereby providing a smooth interface between the Al-SiC composites (Figures 17(b) through (d)). Also the addition of Si improves the thermal conductivity and reduces the CTE of the composites. The thermal and mechanical properties of the composites are affected by porosities, where poor wettability between the matrix and reinforcement can be one of the reasons behind it.[105] The addition of Si in the liquid metal helps in reducing the viscosity of the melt thereby improving the wettability between the matrix and the reinforcement, resulting in smooth penetration during infiltration.[106] Si content less than 6 wt pct and Mg content less than 4 wt pct results in poor thermomechanical properties due to poor wettability between matrix and reinforcement. Formation of brittle intermetallic compound such as Al_3Mg_2 is reported by the addition of magnesium more than 4.7 by mass percent, which wanes the properties of the final composites.[59]

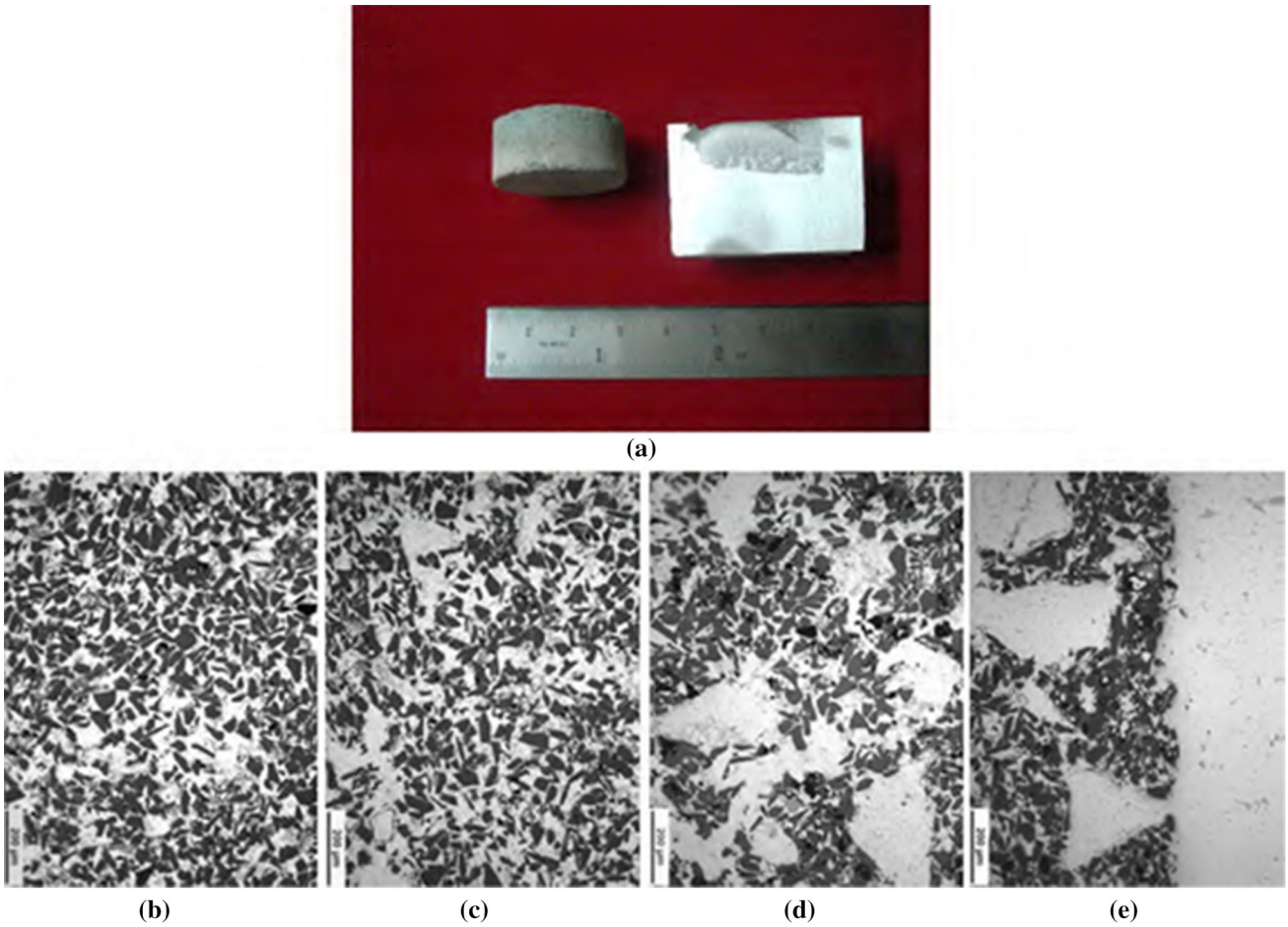

Fig. 13—Images of (*a*) macrograph of graded preform and aluminum-SiC-infiltrated composite specimen. Microstructures of functionally graded Al (6061)-SiCp composite produced by squeeze infiltration: (*b*) starting from outer layer, (*c*) middle layer, (*d*) inner layer in 12-mm-thick casting, and (*e*) interface region.[85]

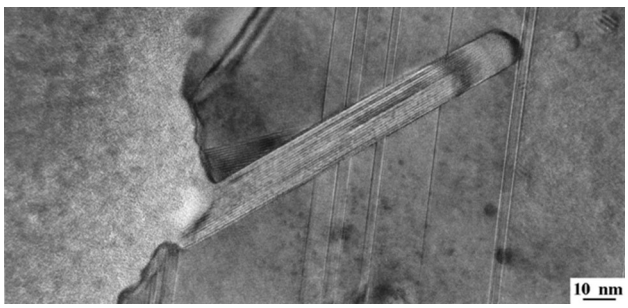

Fig. 14—HRTEM images of Al_4C_3 grains as lath-type morphology. Reprinted from Lancin *et al.*[99] with permission from Elsevier Limited.

The thermal conductivity was more influenced by the interfacial reactions between matrix and reinforcement. Lee *et al.* investigated the effect of Al_4C_3 formation on thermal conductivity (TC) of carbon fiber-reinforced aluminum matrix composites and found that there is considerable decrease in thermal conductivity with increase in Al_4C_3 formation. The main reason for decrease in TC was the surface damages to the carbon fibers (Figure 18) due to the growth of Al_4C_3.[107] The formation of AlN phase from the reactive infiltration of Al/Al alloys into porous α-Si_3N_4 preforms shows great impact on the thermal conductivity (TC) and CTE of the composites. Kalemtas *et al.* suggests that the connectivity of reactive phases (AlN), porosity in the composite, particle size of ceramic phase, and intrinsic properties of the ceramic phase are some of the factors markedly affects the TC and CTE of the composite. Nonuniform distribution of the major phases like AlN, Si, and Al reduces the connectivity of phases which reduces the thermal conductivity of the material.[108] Similarly decrease in the particle size of the ceramic phase increases the grain boundary volume which increases the scattering of conductive electrons leading to low thermal conductivity of the material.[109] The CTE value for AlN is very low and its uniform distribution in the material reduces the usage of Al phase during the process of thermal expansion.

C. *Mechanical Properties*

The mechanical properties of the composite are determined to study the effects of the type of reinforcement used, chemical composition of matrix alloy, infiltration processing temperature, and the interfacial

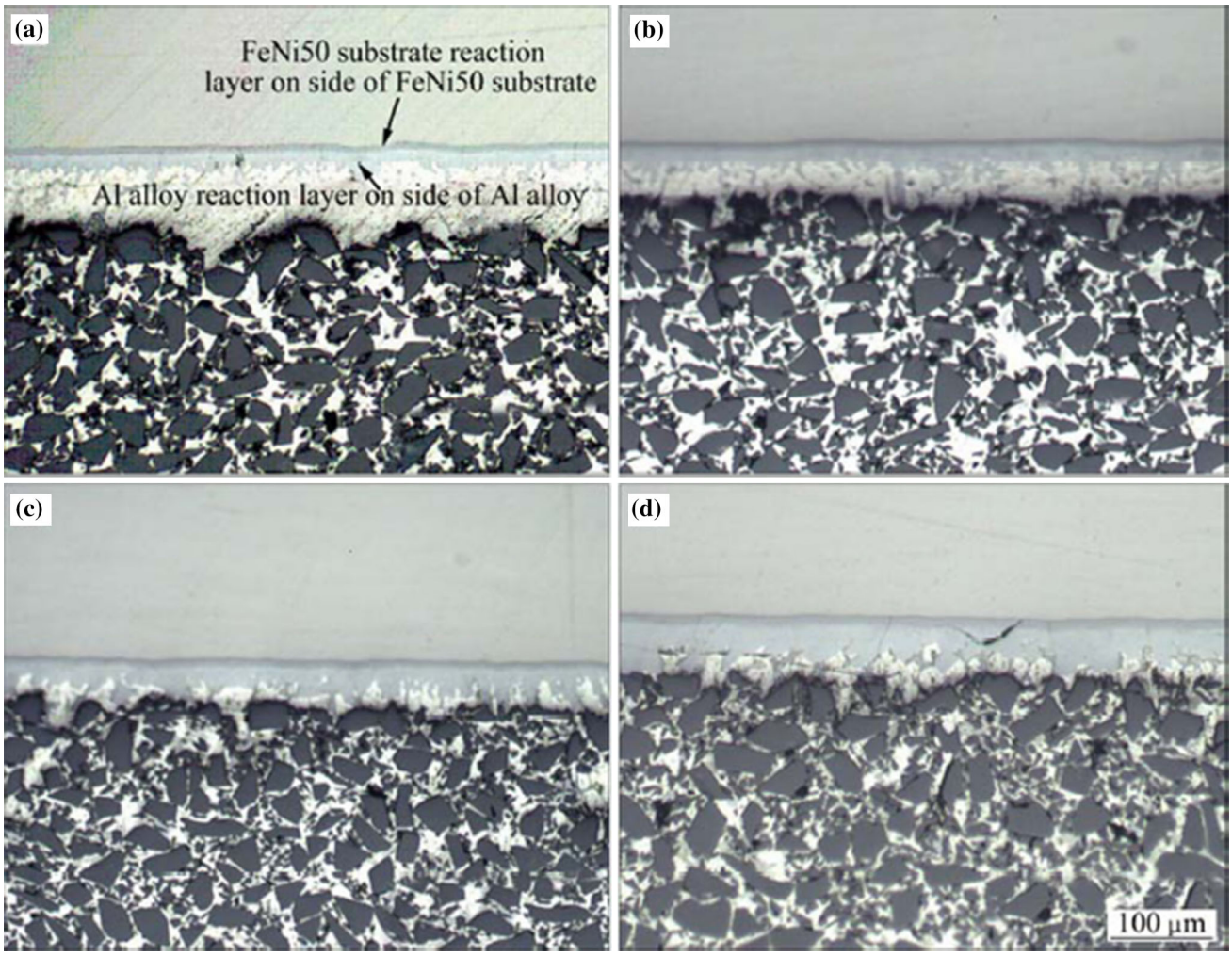

Fig. 15—Effect of infiltration temperature on the thickness of the interfacial reaction layer: (*a*) 943 K (670 °C), (*b*) 963 K (690 °C), (*c*) 983 K (710 °C), and (*d*) 1003 K (730 °C). Reprinted from Chun-xue *et al.*[90] with permission from Elsevier Limited.

reactions. The reinforcement with finer particle size imparts additional interface area assisting the nucleation sites for the grain formation during infiltration process. Obviously developed composite dispenses restrictions to the following factors like plastic flow during deformation, grain growth during heat treatment and dislocation, resulting in higher mechanical strength.[110] Mechanical properties of the composite processed by infiltration technique also depend on the technique adopted for infiltrating molten metal into the preform. Mechanical properties will be less for pressure-less and low pressure infiltration techniques when compared to squeeze infiltration technique, since it offers lower infiltration time which circumvent the growth of interfacial reaction products. Due to the properties like ultrahigh temperature ablation, strength retention at elevated temperatures, excellent thermal stability, and moderate thermal expansion, ZrC particle-reinforced tungsten composites (ZrC/W) had gained much attention in the aerospace applications.[111] Dense ZrC/W matrix composite fabricated by Zhao *et al.* under reactive infiltration of melted Zr_2Cu alloy into a porous WC preform provides mechanical properties, which are similar to the properties of ZrC/W composites prepared by other processing technique like hot-pressing and reactive sintering. $Zr_xCu_yC_z$ nanoparticles formed at the grains of ZrC due to the dissolution Cu in the ZrC matrix act as a pinning point for dislocations (Figure 19) and cracks thereby changing the direction of crack propagation, resulting in high fracture toughness and fracture strength.[112]

The infiltration time also plays a major role on the mechanical properties of metal matrix composites. Tong *et al.* investigated the effect of infiltration time on the mechanical properties of the C/C-SiC composite and found that the reaction between the infiltrated molten metal and carbon preform is time dependent and the preform with higher porosity shows inferior mechanical properties (Figure 20). More the preform porosity more will be the melt and fiber contacts and thus more will be the interfacial reactions with an increase in infiltration time, which will negatively affect the mechanical strength of the composite.[113] An increased mechanical strength can be achieved by reducing the infiltration time thereby avoiding the formation of interfacial phases. The flexural strength of an infiltrated composite

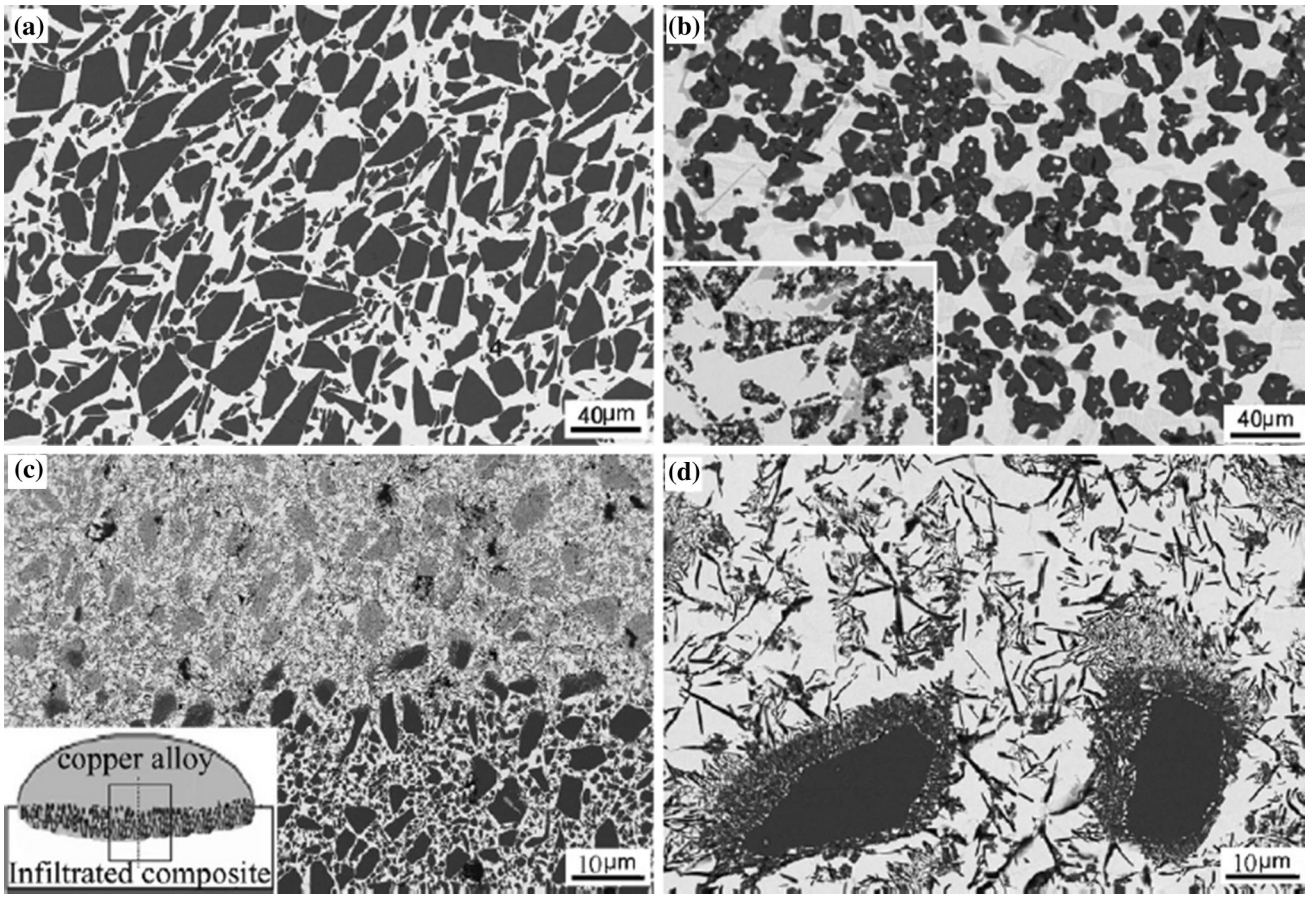

Fig. 16—Microstructure of SiCp/Cu composite: (*a*) infiltrated at 1698 K (1425 °C) for 1 h, (*b*) infiltrated at 1723 K (1450 °C) for 2 h, (*c*) cross section of the interface region, and (*d*) higher magnification of the region (c) in which SiC particles gets melted at an infiltration temperature of 1723 K (1450 °C). Reprinted from Lin *et al.*[94] with permission from Elsevier Limited.

depends more on their fiber matrix interface and porosity. Heat treatment temperatures also have a great influence on the flexural strength of the composites. Higher heat treatment temperature will lead to decrease in flexural strength and elastic modulus due to the volatilization of residual metal.[114] Elastic modulus can also be enhanced by increasing the Si content in the matrix (Al) but heat treatment can provide appreciable improvement in hardness.[115,116] The composite having matrix material with high Cu content can provide better elastic properties and bending strength.[117] Another factor that adversely affects the mechanical strength is that the preform materials contact with each other especially carbon fiber–carbon fiber contact in the case of carbon fiber-reinforced composites. Increase in fiber volume fraction will lead to more and more direct fiber contacts and thus less tensile strength.[118] In a study done by Schlenther *et al.*,[119] it was reported that the impact toughness of MMCs depends on the reinforcement particle size. Finer the particle size lower will be the impact toughness due to lower interparticle distance. Use of coarse reinforcements will provide more interparticle distance leading to large interface area for good bonding between the matrix and reinforcement, so that crack propagation will be over the matrix material which provides energy in the form of plastic deformation before fracture, as a result crack branching occurs (Figure 21). However, increase in the particle diameter leads to increasing the possibility of particle cracking.[120]

Additionally, several investigations suggested that some of the intermetallic phases flourished at the interface during infiltration process had the ability to enhance the hardness of the composite. Sanchez *et al.* inferred from their studies that during centrifugal infiltration process, nickel coated on the carbon fiber gets dissolved in the matrix to form Al_3Ni hard intermetallic compounds, which increase the hardness of the system. They also concluded that the hardness of the composite, in addition, depends on the volume fraction of the reinforcement.[54]

D. *Tribology and Corrosion Behavior*

The tribological property of the composites developed using the infiltration process is directly proportional to the size of the particle and the volume fraction of the reinforcement used. While considering an example, larger ceramic particles will exhibit superior wear resistance but inferior mechanical properties to those containing smaller particles.[121] Zhang *et al.* also studied the effect of porosity in composites prepared

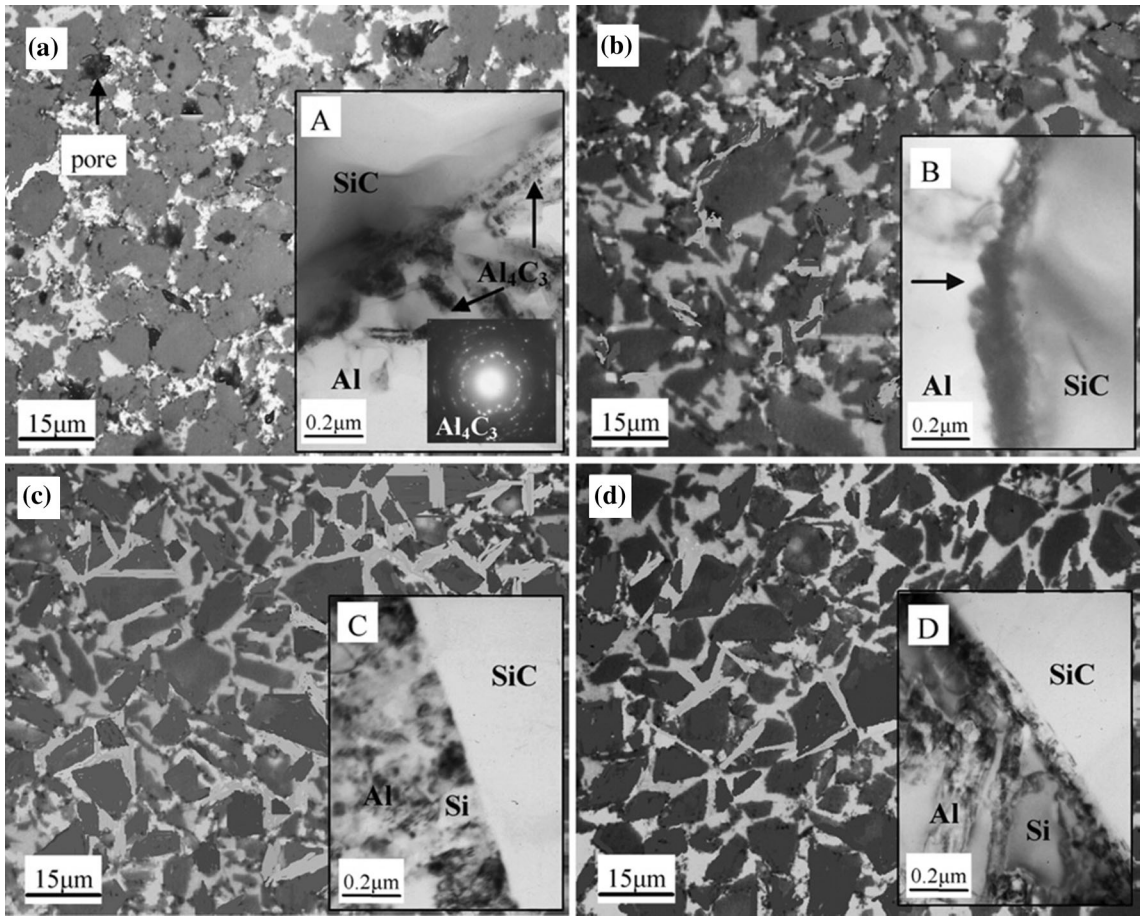

Fig. 17—Optical and TEM images of the interface between Al-SiC composite with the addition of Si: (*a* and A) 0 wt pct, (*b* and B) 6 wt pct, (*c* and C) 12 wt pct, and (*d* and D) 18 wt pct to reduce the interfacial reactions. Reprinted from Shubin *et al.*[104] with permission from Elsevier Limited.

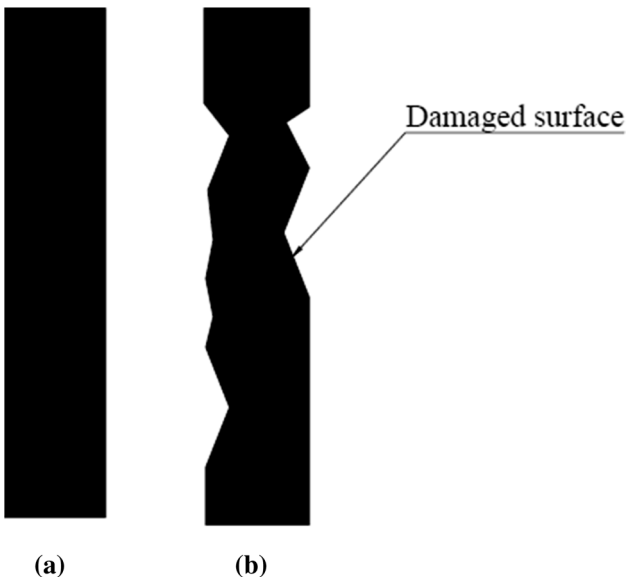

Fig. 18—Change in the diameter of carbon fiber due to the formation of aluminum carbide: (*a*) before aluminum carbide formation and (*b*) after aluminum carbide formation.

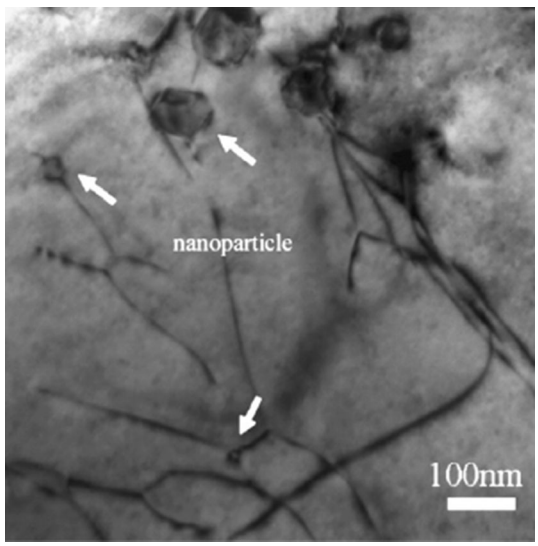

Fig. 19—Dislocation pinning by the intragranular nanoparticles in the ZrC matrix. Reprinted from Yan *et al.*[112] with permission from Elsevier Limited.

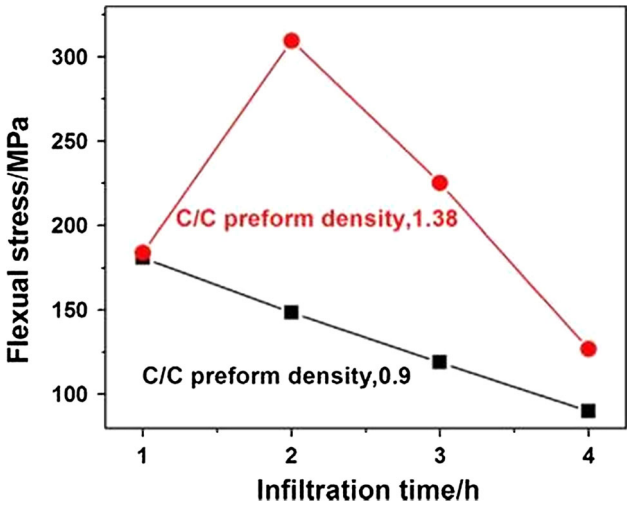

Fig. 20—Flexural strength of C/C-SiC composites prepared in different infiltration time. Reprinted from Yonggang *et al.*[113] with permission from Elsevier Limited.

by pressure-less infiltration of liquid copper into SiC preform and found that porosity has a significant influence on wear resistance. More the amount of porosity less will be the wear resistance and composite with low porosity showing remarkable wear resistance when compared to those with higher porosity.[122] Many investigations are already done on tribological behavior of carbon fiber-reinforced metal matrix composites processed by infiltration technique. The carbon fibers are milled into very fine particles and get squeezed in between the sliding surfaces to form a tribo-layer or a solid lubricant layer.[123] Metal matrix composites containing carbon nanotubes also exhibit better wear resistance properties and the composite shows decreasing effect of wear rate with increase in CNT volume fraction.[124] Chang *et al.*[125] studied the wear behavior of composites processed by infiltrating Al-8 pct Mg into Al_2O_3 preform and found that the wear behavior is governed by foam density and cell size of preform (Figure 22). Composite with lower foam density shows more wear rate when compared to that with higher foam

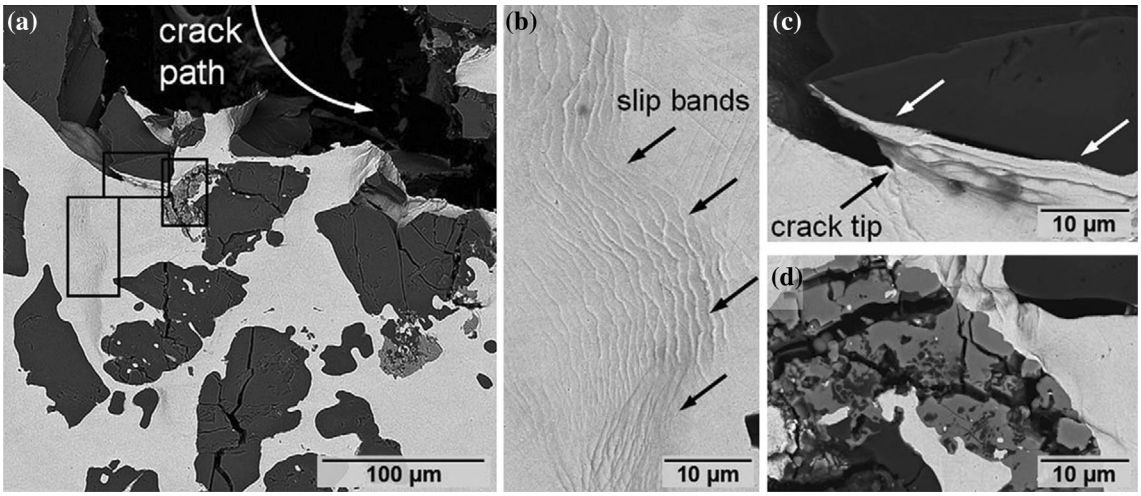

Fig. 21—SEM images of the composite showing: (*a*) crack propagate through particle, (*b*) plastic deformation in the matrix zone, (*c*) good interfacial bonding between the particle and the matrix due to interparticle distance, and (*d*) Severe crack propagation without any plastic deformation in fine particles or agglomerated zone due to lower interparticle distance. Reprinted from Schlenther *et al.*[119] with permission from Elsevier Limited.

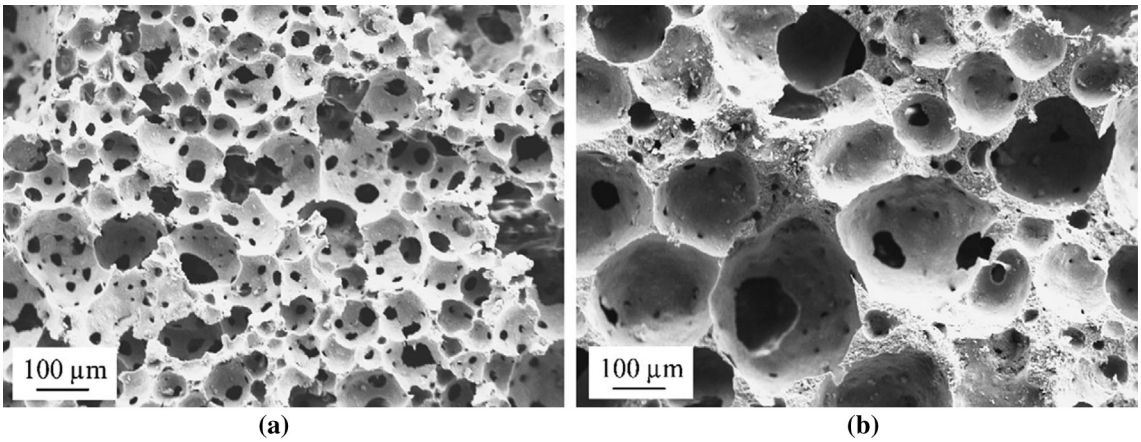

Fig. 22—SEM images of (*a*) Al_2O_3 prefrom having 15 pct density with ~50 to 100 μm cell size and (*b*) Al_2O_3 prefrom having 27 pct density with ~150 to 200 μm cell size. Reprinted from Hong *et al.*[125] with permission from Elsevier Limited.

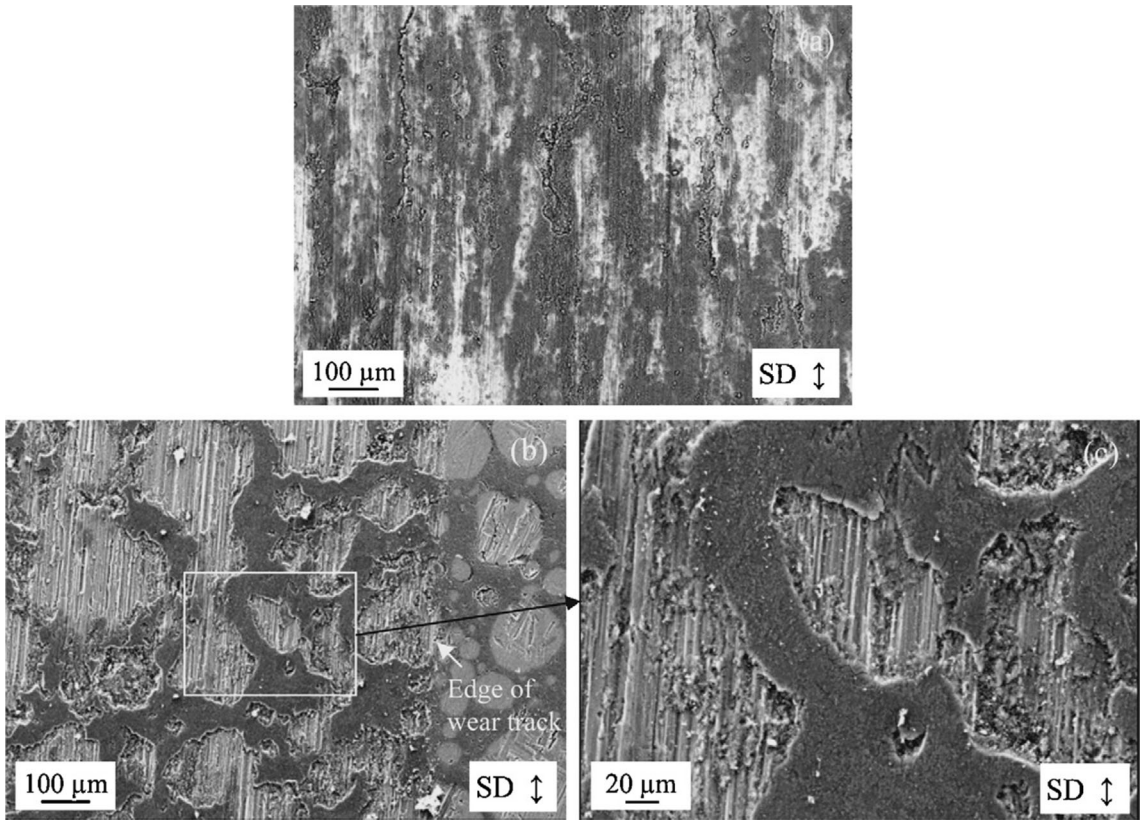

Fig. 23—SEM images of worn out surface of infiltrated composite developed from (*a*) Al_2O_3 preform having 15 pct density with ~50 to 100 μm cell size and (*b* and *c*) Al_2O_3 preform having 27 pct density with ~150 to 200 μm cell size. Reprinted from Hong *et al.*[125] with permission from Elsevier Limited.

density due to the increase in the contact area of the infiltrated matrix with the counter disk during sliding (Figure 23(a)). Increasing the cell size of the preform forms large ridges of Al_2O_3 (Figures 23(b) and (c)) throughout the composite, which prevents the direct wearing of matrix alloy by counter surface.

Dobrzanski *et al.*[126] stated that increase in volume fraction of the reinforcement in composite materials improves the general and pitting corrosion resistance. The higher volume content of the reinforcement phase (surface of the part undergoing testing) does not allow the current to conduct thus retarding electrochemical corrosion. The formation of intermetallic phases during processing, alloying element in the matrix, volume fraction, and the type of reinforcements are the pivotal features affecting the corrosion properties of the composite. The brittle intermetallic phases like Mg_2Si can have the tendency to act as anodic region to the matrix leading to the catastrophic localized corrosion. Escalera *et al.* studied the corrosion behavior of hybrid SiC/fly ash composites infiltrated with Al-8Si-15Mg and Al-3Si-15Mg (wt pct) as matrix alloys. The composite infiltrated with Al-8Si-15Mg results in the formation of Mg_2Si precipitation, which leads to the degradation of materials (Figure 24) due to the aggressive localized corrosion when exposed to ambient atmosphere for certain period. The composite infiltrated with Al-3Si-15Mg reveals no physical degradation even when exposed to humid environment for long duration (Figure 25) due to the termination of Mg_2Si phase, as the silicon content was low enough for the precipitation.[127] At the same time, some studies show that the reinforcement with small mean diameter and addition of Mg in matrix metal during pressure-infiltrated composite enhances the corrosion resistance of the material when exposed to longer duration in NaCl. The formation of reaction products like Mg_2Si at the intersection of the reinforcements blocks the continuity of the metal matrix in the inner side of the developed composite through which the pitting during corrosion propagates and the concentration of interfacial reaction products in smaller reinforcements will be high due to their increased surface area contact with the melt.[128–130] The studies on corrosion behavior of infiltrated composites have shown varying nature of corrosion resistance by different investigators. Hence a detailed investigation is further necessary to generalize the corrosion nature.

VII. APPLICATIONS

Recognizing the ability of liquid metal infiltration processes to assist in the further development of MMC components for aerospace, automotive, defense, electronics packaging, and in general engineering sectors, significant extent of research work is being carried out worldwide. Aluminum matrix composites with high

volume fraction ceramic particles synthesized by infiltration process find potential application as integrated heat sinks and microprocessor lids in electronic packaging.[131] Properties like high thermal conductivity and low thermal expansion coefficient make aluminum nitride (AlN)-reinforced aluminum matrix composites suitable for substrate and packaging applications in microelectronic sector. Low coefficient of thermal expansion makes the composite suitable for lightweight structural parts and heat sink applications.[132] Electronic packaging components with high volume fraction of reinforcement used in thermal management applications minimize the thermal stresses generated by the thermal expansion mismatch between them by dispelling the heat induced from the semiconductor.[133] The automotive industry has successfully implemented liquid metal infiltration technique to develop components like pistons,[134] clutch disk,[135] engine blocks with integral MMC piston liners,[136] *etc.* by Al/SiC and Al/Al_2O_3 composites (Figures 26(a) through (c)). The potential automotive components fabricated using infiltration processes are given in Table I.

Honda manufactures have developed aluminum engine block using cylindrical hybrid preform of short alumina and carbon fibers by squeeze infiltration

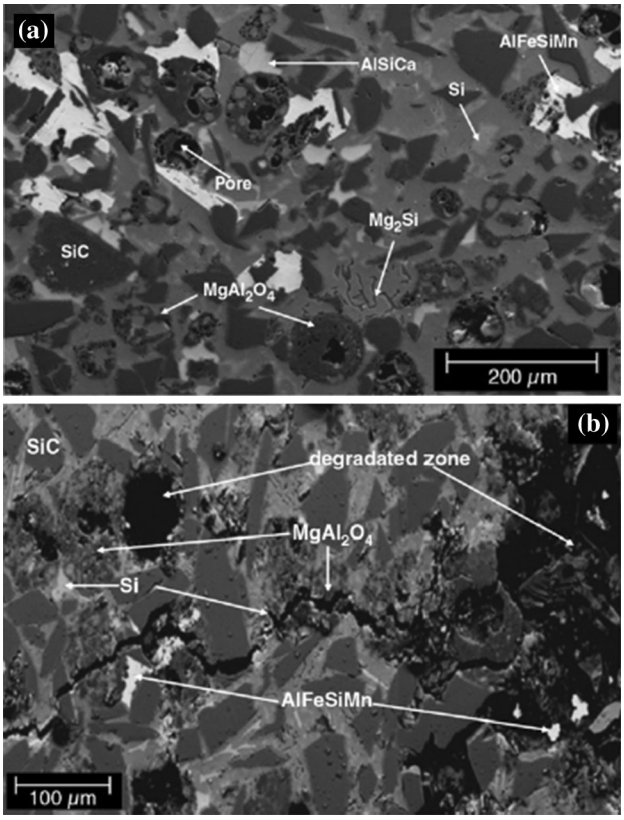

Fig. 24—SEM micrographs of composite infiltrated with Al-8Si-15 Mg as alloy: (*a*) after processing and (*b*) after exposure to ambient atmosphere for 1 month. Reprinted from Escalera *et al.*[127] with permission from Elsevier Limited.

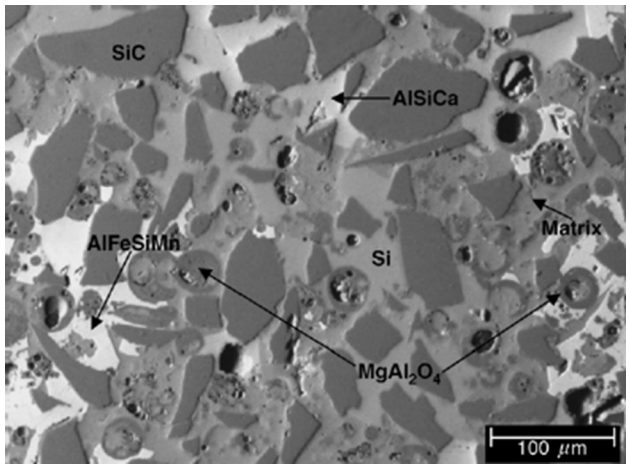

Fig. 25—SEM micrograph of composite infiltrated with Al-3Si-15Mg as alloy after exposure for 11 months in humid environment. Reprinted from Escalera *et al.*[127] with permission from Elsevier Limited.

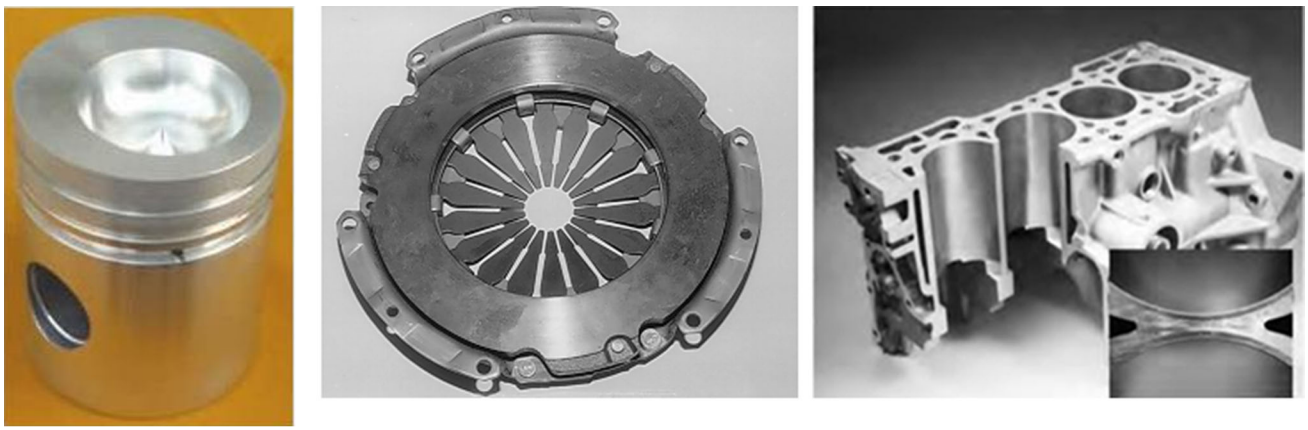

(a) (b) (c)

Fig. 26—(*a*) Diesel engine piston selectively reinforced at the top ring groove area by infiltration process,[134] (*b*) automotive clutch disk manufactured by preform infiltration of aluminum using High Pressure Die Casting (HPDC),[135] and (*c*) cross section of Honda engine block with integral MMC piston liners fabricated by infiltration process. Reprinted from Campbell[136] with permission from ASM International.

process thereby replacing the commercial cast iron engine blocks thus providing weight reduction and higher performance.[137] Coal/lignite fly ash-reinforced aluminum matrix composite made by pressure infiltration technique is a prime material for wear applications.[138] AlSi7Mg with 20 volume percentage SiC particles, liquid AlSi9Mg alloy infiltrated in Al_2O_3 preform by squeeze infiltration are quite worthy for brake disks and piston head of internal combustion engine, respectively.[139] Short alumina fiber-reinforced aluminum matrix composites processed by squeeze infiltration technique is widely used in pistons.[131] Molten metal infiltration of particle-reinforced aluminum matrix composites such as B_4C, SiC, TiC, TiB_2, Al_2O_3 *etc*. are successfully used as components in opto-mechanical assemblies and aerospace applications. Boron carbide, because of its high hardness and other magnificent mechanical properties like low density, high impact and wear resistance, excellent resistance to chemical agents, high melting point, and high capability for neutron absorption, finds application in structural neutron absorber, substrate material for computer hard disk, and as armor plate materials. It is tough to fabricate dense B_4C materials for industrial applications because of its high sensitivity to brittle fracture. This problem can be overcome by the fabrication of B_4C-reinforced aluminum matrix composites by infiltration process. For example in the case of neutron-shielding applications aluminum matrix provides fracture toughness and strength to the composites while boron carbide absorbs neutron.[140] AMC with 40 vol pct SiC particles is used as flight control hydraulic manifolds and the aerospace application further extends to fuel access cover door, ventral fins, fan exit guide vane in the gas turbine engine, rotating blade sleeves in helicopters, *etc*. Particle-reinforced aluminum matrix composites also show their ingenuity in developing braking system of trains and cars and it also find extensive automotive applications such as gear parts, valves, crankshafts, and suspension arms.[131] Table II summarizes the major industries producing components by infiltration process.[141]

Table I. Aluminum-Infiltrated Components Developed and Used in Automobiles

Composite System	Automotive Component	Manufacturer
Al-$Alumina_{(f)}$	diesel engine piston	Toyota
Al-$Al_2O_{3(sf)}$-$C_{(sf)}$	engine	Honda
Al-$FP_{(CF)}$	connecting rod	Du-pont
Al-$SUS_{(CF)}$	connecting rod for petrol engine	Honda
Al-$SiC_{(W)}$	diesel engine piston	Niigata
Al-$SiC_{(w)}$	connecting rod	Nissan
Al-$Alumina_{(f)}$	piston ring grove	Toyota

Table II. The Major Companies Producing Components by Infiltration Process[141]

Sl. No.	Industries Manufacturing MMC by Infiltration
1.	3M Company, Specialty Fibers and Composites (www.3M.com/mmc)
2.	CPS Technologies (http://www.alsic.com/)
3.	Ford Motor Company (www.ford.com)
4.	General Motors (www.gm.com)
5.	Honda Motor Company, Ltd, Japan (www.honda.com)
6.	M-Cubed Technologies, Inc (www.mmmt.com)
7.	Mazda Motor Corporation, Japan
8.	Metal Matrix Cast Composites (MMCC) (www.mmccinc.com)
9.	Motorola, Inc (www.motorola.com)
10.	Porsche, Germany (www.porsche.com)
11.	Toyota Motor Corporation, Japan (http://www.toyota.com/)
12.	Triton Systems Inc (www.tritonsys.com)
13.	Thermal Transfer Composites, LLC (http://www.thermaltc.com/)

VIII. CONCLUSIONS

Liquid metal infiltration of ceramic preform is an effective technique to fabricate MMCs and FGM than other conventional techniques. They offer the advantages like formation of near net shape components, high volume fraction, and uniform distribution of the reinforcement in the liquid matrix phase. Effective liquid metal infiltration in the predesigned preforms can be realized through techniques such as spontaneous infiltration, gaseous infiltration, squeeze infiltration, and vacuum infiltration for the successful fabrication of MMC and FGM components. These techniques have been successfully utilized worldwide and also in CSIR-NIIST, Trivandrum, India to make high-quality Al alloy matrix composites and FGM using carefully optimized process parameters. Composites exhibiting high level of homogeneity in reinforcement distribution, dense and pore free microstructure have been successfully synthesized for industrial applications. As the processing parameters vary from system to system, there is a wide scope to optimize these parameters for different matrix materials and preforms and efforts are on that direction. New engineering components which require higher reinforcement content with better thermal and wear resistance properties and also requiring location-specific properties can be developed by infiltration techniques.

ACKNOWLEDGMENT

The authors are grateful to the CSIR for funding and the Director and Members of Materials Science and Technology Division, CSIR-NIIST, Trivandrum

for their support and encouragement. We are grateful to Mr. Akhil M.G. for helping in drawings.

REFERENCES

1. D.T. Kountouras, C.A. Vogiatzis, F. Stergioudi, A. Tsouknidas, and S.M. Skolianos: *J. Mater. Eng. Perform.*, 2014, vol. 23, pp. 2015–19.
2. K. Naplocha, A. Janus, J.W. Kaczmar, and Z. Samsonowicz: *J. Mater. Process. Technol.*, 2000, vol. 106, pp. 119–22.
3. M. Scheffler and P. Colombo: *Cellular Ceramics: Structure, Manufacturing, Properties and Applications*, Wiley, Weinheim, 2005, p. 645.
4. Paolo. Colombo: *Philos. Trans. R. Soc. A*, 2006, vol. 364, pp. 109–24.
5. P. Colombo and J.R. Hellmann: *Mater. Res. Innov.*, 2002, vol. 6, pp. 260–72.
6. P. Sepulveda: *Am. Ceram. Soc. Bull.*, 1997, vol. 76, pp. 61–65.
7. L. Montanaro, Y. Jorand, G. Fantozzi, and A. Negro: *J. Eur. Ceram. Soc.*, 1998, vol. 18, pp. 1339–50.
8. J. Luyten, I. Thijs, W. Vandermeulen, S. Mullens, B. Wallaeys, and R. Mortelmans: *Adv. Appl. Ceram.*, 2005, vol. 104, pp. 4–8.
9. Y.W. Kim, S.H. Kim, C. Wang, and C.B. Park: *J. Am. Ceram. Soc.*, 2003, vol. 86, pp. 2231–33.
10. T.J. Fitzgerald, V.J. Michaud, and A. Mortensen: *J. Mater. Sci.*, 1995, vol. 30, pp. 1037–45.
11. A.R. Studart, U.T. Gonzenbach, E. Tervoort, and L.J. Gauckler: *J. Am. Ceram. Soc.*, 2006, vol. 89, pp. 1771–89.
12. N. Samer, J. Andrieux, B. Gardiola, N. Karnatak, O. Martin, H. Kurita, L. Chaffron, S. Gourdet, S. Lay, and O. Dezellus: *Compos. A*, 2015, vol. 72, pp. 50–57.
13. M. Rosso: Ceramic and metal matrix composites: route and properties, *12th international scientific conference on Achievements in Mechanics and Materials Engineering*, 2003.
14. B. Chen, S. Li, H. Imai, L. Jia, J. Umeda, M. Takahashi, and K. Kondoh: *Compos. Sci. Technol.*, 2015, vol. 113, pp. 1–8.
15. H. Dieringa: *J. Mater. Sci.*, 2011, vol. 46, pp. 289–306.
16. T. Yamanaka, Y.B. Choi, K. Matsugi, O. Yanagisawa, and G. Sasaki: *J. Mater. Process. Tech*, 2007, vols. 187–188, pp. 530–32.
17. A. Rodriguez-Guerrero, S.A. Sanchez, J. Narciso, E. Louis, and F. Rodriguez-Reinoso: *Acta Mater.*, 2006, vol. 54, pp. 1821–31.
18. L.A. Dobrzański, M. Kremzer, A. Nagel, and B. Huchler: *JAMME*, 2006, vol. 18, pp. 71–74.
19. E.C. Hammel, O.L.-R. Ighodaro, and O.I. Okoli: *Ceram. Int.*, 2014, vol. 40, pp. 15351–70.
20. P. Putyra, P. Kurtyka, L. Jaworska, M. Podsiadlo, and B. Smuk: *AMSE*, 2008, vol. 33, pp. 97–100.
21. O. Raddatz, G.A. Schneider, and N. Claussen: *Acta Mater.*, 1998, vol. 46, pp. 6381–95.
22. A. Mortensen: Comprehensive Composite materials, 2000, vol. 3.20, pp. 521-554.
23. A.M. Zahedi, H.R. Rezaie, J. Javadpour, M. Mazaheri, and M.G. Haghighi: *Ceram. Int.*, 2009, vol. 35, pp. 1919–26.
24. B. Srinivasa Rao and V. Jayaram: *Acta. Mater*, 2001, vol. 49, pp. 2373–85.
25. M.I. Pech-Canul, R.N. Katz, and M.M. Makhlouf: *J. Mater. Process. Technol.*, 2000, vol. 108, pp. 68–77.
26. K.B. Lee and H. Kwon: *Scripta Mater.*, 1997, vol. 36, pp. 847–52.
27. M. Rodríguez-Reyes, M.I. Pech-Canul, J.C. Rendón-Angeles, and J. López-Cuevas: *Compos. Sci. Technol.*, 2006, vol. 66, pp. 1056–62.
28. K.B. Lee, J.H. Choi, and H. Kwon: *Met. Mater. Int.*, 2009, vol. 15, pp. 33–36.
29. M. Guedes, J.M.F. Ferreira, L.A. Rocha, and A.C. Ferro: *Ceram. Int.*, 2011, vol. 37, pp. 3631–35.
30. F. Ortega-Celaya, M.I. Pech-Canul, and M.A. Pech-Canul: *J. Mater. Process. Technol.*, 2007, vol. 183, pp. 368–73.
31. A.M. Bahraini, T. Minghetti, M. Zoellig, J. Schubert, K. Berroth, C. Schelle, T. Graule, and J. Kuebler: *Compos. A*, 2009, vol. 40, pp. 1566–72.
32. K. Lemster, T. Graule, and J. Kuebler: *Mat. Sci. Eng. A*, 2005, vol. 393, pp. 229–38.
33. D. Wittig, A. Glauche, C.G. Aneziris, T. Minghetti, C. Schelle, T. Graule, and J. Kuebler: *Mat. Sci. Eng. A*, 2008, vol. 488, pp. 580–85.
34. A. Contreras, V.H. Lopez, and E. Bedolla: *Scripta Mater.*, 2004, vol. 51, pp. 249–53.
35. B.C. Pai, G. Ramani, R.M. Pillai, and K.G. Satyanarayna: *J. Mater. Sci.*, 1995, vol. 30, pp. 1903–11.
36. G.H. Schiroky, D.V. Miller, M.K. Aghajanian, and A.S. Fareed: *Key Eng. Mater.*, 1997, vols. 127–131, pp. 141–52.
37. H. Nakae and Y. Hiramoto: *Int. J. Metalcast.*, 2011, vol. 5, pp. 23–28.
38. T.P.D. Rajan, R.M. Pillai, and B.C. Pai: *J. Mater. Sci.*, 1998, vol. 33, pp. 3491–503.
39. X.M. Xi and X.F. Yang: *J. Am. Ceram. Soc.*, 1996, vol. 79, pp. 102–08.
40. R.Y. Lin, R.J. Arsenault, G.P. Martins, and S.G. Fishman: *Interfaces in Metal-Ceramic Composites*, Minerals, Metals and Materials Society, Warrendale, PA, 1990, p. 291.
41. G. Mingyuan, J. Yanping, M. Zhi, W. Zengan, and W. Renjie: *Mater. Sci. Eng. A.*, 1998, vol. 252, pp. 188–98.
42. Idem. Jpn. Kokai. Tokkyo. Koho. JP 01279721 A2, 10 Nov, 1989, Heisei, pp.13.
43. R.K. Dwivedi, V. Irick Jr, US patent 4871008, 1989.
44. P.K. Rohatgi, J.K. Kim, N. Gupta, S. Alaraj, and A. Daoud: *Compos. A*, 2006, vol. 37, pp. 430–37.
45. E. Carreno-Morelli, T. Cutard, R. Schaller, and C. Bonjour: *Mater. Sci. Eng. A*, 1998, vol. 251, pp. 48–57.
46. L.H. Qi, L.Z. Su, J.M. Zhou, J.T. Guan, X.H. Hou, and H.J. Li: *J. Alloy. Compd.*, 2012, vol. 527, pp. 10–15.
47. A. Demir and N. Altinkok: *Compos. Sci. Technol.*, 2004, vol. 64, pp. 2067–74.
48. T. Joseph Blucher: *J. Mater. Process. Technol.*, 1992, vol. 30, pp. 381–90.
49. Z. Wang, X. Zhifeng, Y. Huan, Q. Yan, and B.W. Xiong: *Adv. Mater. Res*, 2013, vols. 634–638, pp. 1914–17.
50. W. Hufenbach, M. Gude, A. Czulak, J. Sleziona, A. Dolata-Grosz, and M. Dyzia: *JAMME*, 2009, vol. 35, pp. 177–83.
51. A. Daoud: *Mater. Sci. Eng. A*, 2005, vol. 391, pp. 114–20.
52. N.W. Rasmussen, P.N. Hansen, and S.F. Hansen: *Mater. Sci. Eng. A*, 1991, vol. 135, pp. 41–43.
53. J. Wannasin and M.C. Flemings: *J. Mater. Process. Technol.*, 2005, vol. 169, pp. 143–49.
54. M. Sanchez, J. Rams, and A. Urena: *Compos. A*, 2010, vol. 41, pp. 1605–11.
55. Y. Nishida, I. Shirayanagi, and Y. Sakai: *Metall. Mater. Trans. A*, 1996, vol. 27, pp. 4163–69.
56. R.M. Andrews and A. Mortensen: *Mater. Sci. Eng. A.*, 1991, vol. 144, pp. 165–68.
57. J. Pan, D.M. Yang, H. Wan, and X.F. Yin: *Key Eng. Mater.*, 1995, vols. 104–107, pp. 275–82.
58. Y. Deming, Y. Xinfang, and P. Jin: *J. Mater. Sci. Lett.*, 1993, vol. 12, pp. 252–53.
59. T. Matsunaga, K. Matsuda, T. Hatayama, K. Shinozaki, and M. Yoshida: *Compos. A*, 2007, vol. 38, pp. 1902–11.
60. T. Matsunaga, K. Ogata, T. Hatayama, K. Shinozaki, and M. Yoshida: *Compos. A*, 2007, vol. 38, pp. 771–78.
61. G. Sasaki, J. Adachi, Y.-B. Choi, J. Pan, T. Fujii, K. Matsugi, and O. Yanagisawa: *Mater. Sci. Forum*, 2005, vols. 475–479, pp. 921–24.
62. F. Gul and M. Acilar: *Compos. Sci.Technol.*, 2004, vol. 64, pp. 1959–70.
63. W.-S. Chung and S.J. Lin: *Mater. Res. Bull.*, 1996, vol. 31, pp. 1437–47.
64. J. Yang and D.D.L. Chung: *J. Mater. Sci.*, 1989, vol. 24, pp. 3605–12.
65. B. Xiong, Y. Huan, X. Zhifeng, Q. Yan, and C. Cai: *J. Alloys Compd.*, 2011, vol. 509, pp. L279–83.
66. O. Beffort, S. Long, C. Cayron, J. Kuebler, and P.-A. Buffat: *Compos. Sci. Technol.*, 2007, vol. 67, pp. 737–45.
67. K. Pradeep Rohatgi, V. Tiwari, and N. Gupta: *J. Mater. Sci.*, 2006, vol. 41, pp. 7232–39.
68. W. Deqing, S. Ziyan, G. Hong, and H.F. Lopez: *J. Mater. Synth. Process*, 2001, vol. 9, pp. 247–51.
69. D. Coupard, J. Goni, and J.F. Sylvain: *J. Mater. Sci.*, 1999, vol. 34, pp. 5307–13.
70. R. Saha, E. Morris, and N. Chawla: *J. Mater. Sci. Lett.*, 2002, vol. 21, pp. 337–39.

71. L.M. Peng and K.S. Han: *J. Mater. Sci. Lett.*, 2003, vol. 22, pp. 279–82.
72. C.P. Ju, K.I. Chen, and J.H. Chern Lin: *J. Mater. Sci.*, 1994, vol. 29, pp. 5127–34.
73. J.-T. Guan, L.-H. Qi, J. Liu, J.-M. Zhou, and X.-L. Wei: *Trans. Nonferrous Met. Soc. China*, 2013, vol. 23, pp. 3173–79.
74. J. Bear: *Dynamics of Fluids in Porous Media*, Dover Publications, New York, 1988.
75. C. Garcia-cordovillaa, E. Louisb, and J. Narciso: *Acta Mater.*, 1999, vol. 47, pp. 4461–79.
76. V. Michaud and A. Mortensen: *Compos. A*, 2001, vol. 32, pp. 981–96.
77. M. Bahraini, J.M. Molina, M. Kida, L. Weber, J. Narciso, and A. Mortensen: *Curr. Opin. Solid. State Mater. Sci.*, 2005, vol. 9, pp. 196–201.
78. V. Sampath, N. Ramanan, and R. Palaninathan: *Mater. Manuf. Process*, 2006, vol. 21, pp. 495–05.
79. A. Papworth and P. Fox: *Mater. Lett.*, 1996, vol. 29, pp. 209–13.
80. T.R. Vijayaram, S. Sulaiman, A.M.S. Hamouda, and M.H.M. Ahmad: *J. Mater. Process. Technol.*, 2006, vol. 178, pp. 34–38.
81. H.A. Alhashmy and M. Nganbe: *Mater. Des.*, 2015, vol. 67, pp. 154–58.
82. K.M. Sree Manu, V.G. Resmi, M. Brahmakumar, N. Anand, T.P.D. Rajan, C. Pavithran, B.C. Pai, and K. Manisekar: *Mater. Sci. Forum*, 2012, vol. 710, pp. 371–76.
83. S.S. Wang: *J. Compos. Mater.*, 1983, vol. 17, pp. 210–23.
84. B. Kieback, A. Neubrand, and H. Riedel: *Mat. Sci. Eng. A*, 2003, vol. 362, pp. 81–106.
85. K.M. Sree Manu, V.G. Resmi, M. Brahmakumar, P. Narayanasamy, T.P.D. Rajan, C. Pavithran, and B.C. Pai: *Trans. Indian. Inst. Metals*, 2012, vol. 65, pp. 747–51.
86. T.Y. Kosolapova: *Carbides Properties, Production and Applications*, Plenum, New York, 1971.
87. F. Delannay, L. Froyen, and A. Deruyttere: *J. Mater. Sci.*, 1987, vol. 22, pp. 1–16.
88. H. Ribes, M. Suery, G. Esperance, and J.G. Legoux: *Metall. Trans. A*, 1990, vol. 21, pp. 2489–96.
89. M.Y. Gu, Z. Mei, Y.P. Jin, and Z.G. Wu: *Scripta Mater.*, 1999, vol. 40, pp. 985–91.
90. C.-X. Ma, J.-K. Yu, C. Xue, and J.-K. Yu: *Chen Xue And Zhi-Qing Zhang: Trans Nonferrous Metal. Soc. China*, 2013, vol. 23, pp. 2229–35.
91. S. Zhang, G. Chen, R. Pei, M. Hussain, Y. Wang, D. Li, P. Wang, and W. Gaohui: *Mater. Des.*, 2015, vol. 65, pp. 567–74.
92. D. Manfredi, M. Pavese, S. Biamino, A. Antonini, P. Fino, and C. Badini: *Compos. A*, 2010, vol. 41, pp. 639–45.
93. N. Nagendra, B.S. Rao, and V. Jayaram: *Mater. Sci. Eng. A*, 1999, vol. 269, pp. 26–37.
94. L. Zhang, X. Qu, B. Duan, X. He, S. Ren, and M. Qin: *Sci. Technol.*, 2008, vol. 68, pp. 2731–38.
95. S.G. Warrier, C.A. Blue, and R.Y. Lin: *J. Mater. Sci. Lett.*, 1993, vol. 12, pp. 865–68.
96. E. Hajjari, M. Divandari, and A.R. Mirhabibi: *Mater. Des.*, 2010, vol. 31, pp. 2381–86.
97. Y.-Q. Ma, L.H. Qi, W.-.Q. Zheng, J.M. Zhou, and L.Y. Ju: *Nonferrous Met. Soc. China*, 2013, vol. 23, pp. 1915–21.
98. Q. Yang, J. Liu, S. Li, F. Wang, and W. Tengteng: *Mater. Des.*, 2014, vol. 57, pp. 442–48.
99. M. Lancin and C. Marhic: *J. Eur. Ceram. Soc.*, 2000, vol. 20, pp. 1493–1503.
100. M.H. Vidal-Sétif, M. Lancin, C. Marhic, R. Valle, J.-C. Daux, and M. Rabinovitch: *Mater. Sci. Eng. A*, 1999, vol. 272, pp. 321–33.
101. L. Qi, J. Luyan, and J. Zhou: *Proc. Eng.*, 2014, vol. 81, pp. 1577–82.
102. L.A. Dobrzanski, M. Kremzer, and A. Nagel: *JAMME*, 2007, vol. 24, pp. 183–186.
103. T. Etter, M. Papakyriacou, P. Schulz, and P.J. Uggowitzer: *Carbon*, 2003, vol. 41, pp. 1017–24.
104. Shubin. Ren, Xinbo. He, Qu. Xuanhui, Islam.S. Humail, and Yan. Li: *Compos. Sci. Technol.*, 2007, vol. 67, pp. 2103–13.
105. H.S. Lee and S.H. Hong: *Mater. Sci. Technol.*, 2003, vol. 19, pp. 1057–64.
106. M.I. Pech-Canul, R.N. Katz, and M.M. Makhlouf: *J. Mater. Process. Technol.*, 2000, vol. 108, pp. 68–77.
107. M. Lee, Y. Choi, K. Sugio, K. Matsugi, and G. Sasaki: *Compos. Sci. Technol.*, 2014, vol. 97, pp. 1–5.
108. A. Kalemtas, G. Topates, O. Bahadir, P.K. Isci, and H. Mandal: *Nonferrous Met. Soc. China*, 2013, vol. 23, pp. 1304–13.
109. X.Y. Qin, B.M. Wu, Y.L. Du, L.D. Zhang, and H.X. Tang: *Nanostruct. Mater.*, 1996, vol. 7, pp. 383–91.
110. S.M. Seyed: *Mater. Des.*, 2006, vol. 27, pp. 216–22.
111. G.M. Song, Y.J. Wang, and Y. Zhou: *J. Mater. Sci.*, 2001, vol. 36, pp. 4625–31.
112. Y.-W. Zhao, Y.-J. Wang, L. Chen, Y. Zhou, G.-M. Song, and J.-P. Li: *Int. J. Refract. Metal. H*, 2013, vol. 37, pp. 40–44.
113. Y. Tong, S. Bai, Q.H. Qin, H. Zhang, and Y. Ye: *Ceram. Int.*, 2015, vol. 41, pp. 4014–20.
114. Y. Zhu, S. Wang, H. Chen, W. Li, J. Jiang, and Z. Chen: *Ceram. Int.*, 2013, vol. 39, pp. 9085–89.
115. S. Ren, X. He, Q. Xuanhui, I.S. Humail, and Y. Li: *Compos. Sci. Technol.*, 2007, vol. 67, pp. 2103–13.
116. X.-F. Tan, F.-H. Zeng, S.-Q. Wang, F. Zhou, and X. Xiong: *Trans. Nonferrous Metal. Soc. China*, 2014, vol. 24, pp. 2359–65.
117. Y. Zhu, S. Wang, H. Chen, W. Li, and Z. Chen: *Ceram. Int.*, 2014, vol. 40, pp. 2793–98.
118. S. Can Kurnaz: *Mater. Sci. Eng. A*, 2003, vol. 346, pp. 108–15.
119. E. Schlenther, C.G. Aneziris, T. Graule, and J. Kuebler: *Mater. Sci. Eng. A.*, 2012, vol. 556, pp. 751–57.
120. C.A. Lewis and P.J. Withers: *Acta Metall. Mater.*, 1995, vol. 43, pp. 3685–99.
121. J.F. Zhang, L.C. Zhang, and Y.W. Mai: *J. Mater. Sci.*, 1995, vol. 30, pp. 1961–66.
122. L. Zhang, X.-H. Qu, B.-H. Duan, X.-B. He, and M.-L. Qin: *Trans. Nonferrous Metal Soc. China*, 2008, vol. 18, pp. 1076–82.
123. A. Daoud: *Mater. Lett.*, 2004, vol. 58, pp. 3206–13.
124. S.-M. Zhou, X.-B. Zhang, Z.-P. Ding, C.-Y. Min, G.-L. Xu, and W.-M. Zhu: *Compos. A*, 2007, vol. 38, pp. 301–306.
125. H. Chang, J. Binner, and R. Higginson: *Wear*, 2010, vol. 268, pp. 166–71.
126. L.A. Dobrzanski, M. Kremzer, and M. Drak: *JAMME*, 2008, vol. 30, pp. 121–28.
127. R. Escalera-Lozano, C.A. Gutiérrez, M.A. Pech-Canul, and M.I. Pech-Canul: *Mater. Charact.*, 2007, vol. 58, pp. 953–60.
128. S. Candan: *Corros. Sci.*, 2009, vol. 51, pp. 1392–98.
129. S. Candan: *Mater. Lett.*, 2004, vol. 58, pp. 3601–05.
130. Z. Ahmad, P.T. Paulette, and B.J.A. Aleem: *J. Mater. Sci.*, 2000, vol. 35, pp. 2573–79.
131. K. Surappa: *Sadhana*, 2003, vol. 28, pp. 319–34.
132. C. Toy and W.D. Scott: *J. Am. Ceram. Soc.*, 1990, vol. 73, pp. 97–101.
133. H.S. Lee and S.H. Hong: *Mater. Sci. Technol.*, 2003, vol. 19, pp. 1057–64.
134. R. Mahadevan and R. Gopal: 68th WFC - World Foundry Congress, 2008, 379.
135. J. Goni, I. Sarries. J. Barcena, M. Garcia de Cortazar, P.Egizabal and J. Coleto: Developments in novel production processes for metal matrix composites, *Proc. 16th International Conference on Composite materials*, Kyoto, Japan, 8 - 13 July 2007.
136. F.C. Campbell: *Lightweight Materials: Understanding the Basics*, Materials Park, Ohio, ASM International, 2012, p. 459.
137. M. Ebisawa, T. Hara, T. Hayashi and H. Ushio: Production Process for Metal Matrix Composite (MMC) Engine Block, SAE Special Paper Series, 910835.
138. G. Itskos, P. K. Rohtagi, A. Moutsatsou, C. Vasilatos, J. D. Defow and N. Koukouzas: Pressure infiltration technique for the synthesis of A356 Al/fly ash composites: microstructure and tribological performance, *World of Coal Ash Conference (WOCA)*, Denver, CO, 2011.
139. W. Wilk and B. Staniewicz-Brudnik: Abrasive Machining of Metal Matrix Composites, *8th International conference Advanced Manufacturing Operations*, 2008, pp.373.
140. B.S. Lee and S. Kang: *Mater. Chem. Phys.*, 2001, vol. 67, pp. 249–55.
141. A. Evans, C. San Marchi, and A. Mortensen: *Metal Matrix Composites in Industry: An Introduction and a Survey*, Springer, New York, 2003.